Statistical Mechanics and Field-Induced Phase Transitions of the Heisenberg Antiferromagnet*

F. Burr Anderson and Herbert B. Callen
Department of Physics and Laboratory for Research on the Structure of Matter, University of Pennsylvania, Philadelphia, Pennsylvania
(Received 24 June 1964)

The spin-flop and flop-para phase transitions of a simple uniaxial antiferromagnet are analyzed by a Green-function analysis. The temperature dependence of the field for antiferromagnetic resonance, the parallel and perpendicular susceptibilities, and the sublattice magnetizations are also computed. It is shown that these effects are sensitive to the temperature-dependent renormalization of spin-wave energies, and this effect is analyzed in some detail. Results are in good semiquantitative agreement with antiferromagnetic resonance in MnF_2 and Cr_2O_3, with the phase transition boundaries in $MnBr_2\cdot 4H_2O$, and with the perpendicular susceptibility of MnF_2.

1. INTRODUCTION

In this paper we discuss the statistical mechanics of a simple uniaxial Heisenberg antiferromagnet, with special emphasis on the nature and temperature dependence of the several phase transition boundaries and of antiferromagnetic resonance (AFMR). We also consider such thermodynamic properties as the sublattice magnetizations and the parallel and perpendicular susceptibilities. The types of materials motivating the investigation are $RbMnF_2$, MnF_2, and Cr_2O_3, which have been studied in the antiferromagnetic phase by AFMR and other methods, and $MnBr_2\cdot 4H_2O$, an antiferromagnet with small exchange field and low Néel temperature, for which the entire phase diagram has been studied by a variety of experimental methods. The conceptual background of the problem and the heuristic significance of the results are discussed respectively in this Introduction and in the final section of the paper, both of which are self-contained.

The mathematical model which forms the basis of discussion consists of a simple cubic or a body-centered cubic[1] array of magnetic ions of spin S, interacting by a negative nearest-neighbor exchange interaction. In addition, we assume the presence of a uniaxial anisotropy[2] and an external magnetic field, each coaxial with the crystalline z axis.

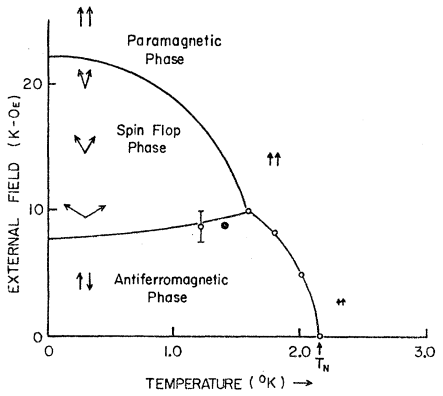

FIG. 1. Phase diagram for $MnBr_2\cdot 4H_2O$, from Schelleng and Friedberg (Refs. 4, 5). The symbol ● indicates a specific-heat anomaly observed by Schelleng, the ○ represents measurements by Tsujikawa and Kanda (points without error bars—Ref. 6) and by Bolger (point with error bar—Ref. 7), by optical absorption. The solid curves are schematic, being computed by molecular field theory scaled to the experimental points.

At a given temperature below the Néel temperature, and at sufficiently small field, the individual spins are aligned parallel or antiparallel to the field (with, of course, random thermal fluctuations around these average directions). As the field increases a phase transition occurs, the spins "flopping" to a generally transverse orientation.[3] As the field increases further, the spins increasingly tilt toward the field direction. At a particular value of the field the average direction of each spin then becomes parallel to the field direction, thereby defining a second phase transition to the paramagnetic phase, as illustrated in Fig. 1 (taken from the measurements of Schelleng[4] and Friedberg[5] on $MnBr_2\cdot 4H_2O$ and of optical absorption measurements[6,7]). We shall be concerned primarily with the antiferromagnetic (low-field) and the paramagnetic (high-field) phases, and with the curves bounding the regions of stability of these phases.

The theoretical interest in the phase transitions centers in the direct relationship of the transitions to the "renormalization" of the spin-wave energies through spin-wave interactions. The role of the renormalization effect is most clearly evident when we consider the flop-

* Supported by the U. S. Office of Naval Research.

[1] These structures have the convenient property of being resolvable into two sublattices such that the nearest neighbors of an ion on one sublattice lie only on the other sublattice.

[2] For a discussion of this model, of the role of the uniaxial anisotropy in establishing a unique ground state, and of the reconcilliation of the uniaxial anisotropy with the otherwise cubic crystal symmetry, see J. Van Kranendonk and J. H. Van Vleck, Rev. Mod. Phys. 30, 1 (1958).

[3] As is very well known the spin-flop transition occurs because the susceptibility is greater in the transverse configuration, and the energy $-\frac{1}{2}\chi^{\perp}H^2$ overcomes the anisotropy energy which tends to keep the spins along the axis of the field.

[4] J. H. Schelleng, Ph.D. thesis, Carnegie Institute of Technology, 1963 (unpublished).

[5] J. H. Schelleng and S. Friedberg (to be published).

[6] I. Tsujikawa and J. Kanda, J. Phys. Radium 20, 352 (1959).

[7] B. Bolger, Communications, Conference de Physique Des Basses Temperatures (1955), p. 244 (unpublished).

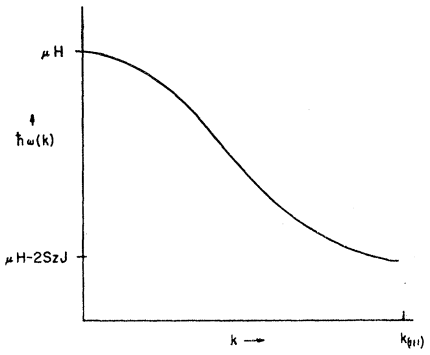

FIG. 2. Spin-wave spectrum in paramagnetic phase at low temperature.

para transition. Above this transition, in the paramagnetic phase, the configuration of the system is identical to that in a ferromagnet. We can therefore adopt the standard spin-wave analysis of the ferromagnet,[8] the spin-wave frequencies being

$$\hbar\omega(\mathbf{k})=\mu H-S[J(0)-J(\mathbf{k})], \tag{1.1}$$

where $J(0)$ and $J(\mathbf{k})$ are the Fourier transforms of the exchange interaction, $\mu=ge\hbar/2mc$, and H is the magnetic field.[9] The minus sign before the second term in Eq. (1.1) has been inserted to take explicit cognizance of the negative sign of the exchange interaction, and it results in an inversion of the spectrum with respect to the usual ferromagnetic case, as indicated in Fig. 2. The minimum of the spin-wave spectrum in a simple cubic structure occurs at the [111] corner of the Brillouin zone,[9] where $k_xa=k_ya=k_za=\pi$ and $\hbar\omega(\mathbf{k}_{111})=\mu H-2SzJ$. Consequently, this spin-wave frequency becomes negative if the magnetic field is less than the critical value $H_c=2SzJ/\mu$. The spin-wave amplitude then grows exponentially, corresponding to an instability in the paramagnetic phase, and a phase transition to the spin-flop phase occurs. However, the simple spin-wave theory just given predicts no temperature dependence of the critical field. But, in fact, the spin-wave frequencies of Eq. (1.1) are renormalized[10] by a temperature-dependent factor $R(T)$, reflecting the effect on the given mode of the presence of other thermally excited spin waves.

$$\hbar\omega(\mathbf{k})=\mu H-S[J(0)-J(\mathbf{k})]R(T), \tag{1.2}$$

whence

$$\mu H_c=2SzJR(T). \tag{1.3}$$

Thus the temperature dependence of the critical-field curve directly reflects the temperature dependence of the spin-wave renormalization.

[8] F. J. Dyson, Phys. Rev. **102**, 1217, 1230 (1956).

[9] The bracketed expression in Eq. (1.1) is simply

$$zJ[1-\tfrac{1}{3}\cos k_xa-\tfrac{1}{3}\cos k_ya-\tfrac{1}{3}\cos k_za]$$

for a simple-cubic nearest-neighbor model, where z is the number of nearest neighbors.

[10] A good discussion of the renormalization effects is given by F. Keffer and R. Loudon, J. Appl. Phys. **32**, 25 (1961).

Whereas the transition from the spin-flop to the paramagnetic phase is second order in the Landau[11] sense (the two phases are indistinguishable at the tranitions), the transition between antiferromagnetic and spin-flop phases is first order (the phases being distinct at the transition). The analysis of this first-order transition is therefore complicated by the possibility of metastable "superheating" and "supercooling" states, analogous to those in a conventional gas-liquid transition. In Fig. 3 we show a conventional P-V isotherm for a gas-liquid transition, and the corresponding H-M isotherm for the spin-flop transition; the ordinate in Fig. 3(b) is taken as $-H$ to preserve the thermodynamic analogy ($-P\leftrightarrow H$) At point A the liquid is locally stable (i.e., the free energy has a local minimum) and the value of the free energy is equal to that in the gas at point D; the pressure $P_A=P_D$ is the pressure of the true first-order transition at temperature T_1, as shown in Fig. 3(c). If the pressure is quasistatically decreased below P_A along the T_1 isotherm in Fig. 3(a), the local minimum of the free energy changes shape, the quadratic terms finally ceasing to be positive definite at the point B. At this point some generalized coordinate finds a vanishing restoring force and the natural frequency of the corresponding dynamical mode vanishes. Thus the point B in Fig. 3(a), and the corresponding curve in Fig. 3(c), demarcate the limit of local stability of the liquid phase.

In the antiferromagnet similar considerations apply, and along the limiting curve of local stability of the antiferromagnetic phase [B in Figs. 3(b) and 3(d)] one of the spin-wave frequencies of the antiferromagnetic phase vanishes. We shall refer to the resulting stability

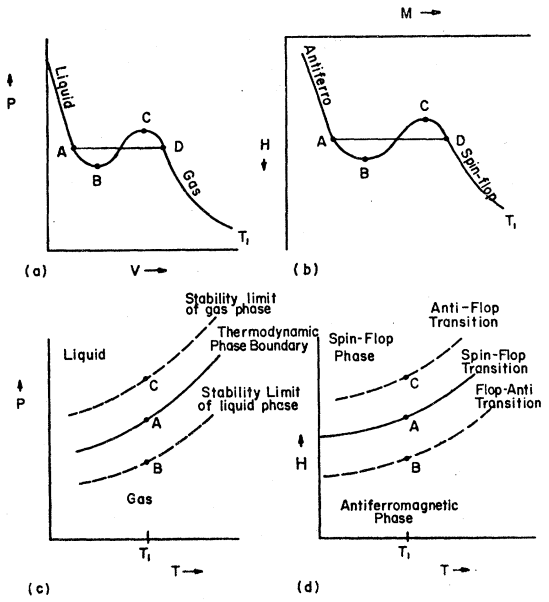

FIG. 3. Phase diagrams for liquid-gas and spin-flop transitions.

[11] See for example L. D. Landau and E. M. Lifshitz, *Statistical Physics* (Pergamon Press, Ltd., London, 1958).

boundary as the "anti-flop" transition curve; this should not be confused with the true "spin-flop" transition curve AD, nor with the "flop-anti" transition curve C which bounds the stability of the spin-flop phase. We shall calculate only the anti-flop transition curve in this paper.

The relationship among the critical fields is most simply illustrated at zero temperature. If the spins are treated as classical vectors, the energy E_{II} in the antiferromagnetic configuration can be directly compared with the energy E_θ in the spin-flop configuration. Based on the model described in the second paragraph of the Introduction [the corresponding Hamiltonian is given in Sec. 2, Eq. (2.1)] one finds

$$E_\theta - E_{II} = \tfrac{1}{2}N[zJS^2\cos 2\theta - 2\mu HS\cos\theta - 2KS^2\cos^2\theta] - \tfrac{1}{2}N[zJS^2 - 2KS^2], \quad (1.4)$$

where K is the anisotropy constant and θ is the angle between the spins and the z axis. Minimizing this expression with respect to the angle θ, we find that the resultant energy difference vanishes for a critical field H_c^0 given by

$$\mu H_c^0 = 2S[K(zJ-K)]^{1/2}. \quad (1.5)$$

A quantum-mechanical treatment would undoubtedly alter the result, and we shall not make quantitative reference to this value of the critical field, indicating it only for purposes of illustration.

The critical field bounding the stability of the spin-flop phase (that is, the flop-anti transition) has been analyzed by Wang and Callen[12] by a spin-wave analysis. They find the critical field

$$\mu H_c^J = 2S(zJ-K\xi^2)\left[\frac{K\xi(1+\xi)}{2zJ+K\xi(1+\xi)}\right]^{1/2}, \quad (1.6)$$

where

$$\xi = (1-1/2S)^{1/2}. \quad (1.7)$$

Finally, the critical field bounding the stability of the antiferromagnetic phase (the anti-flop transition) follows from the standard[13–15] spin-wave treatment of the antiferromagnetic phase. There are two spin-wave branches, with energies

$$\pm\mu H + 2S[K\xi^2(zJ+K\xi^2)]^{1/2}, \quad (1.8)$$

and the mode of zero wave vector, in the lower branch, becomes unstable at the critical field

$$\mu H_c^a = 2S[K\xi^2(zJ+K\xi^2)]^{1/2}. \quad (1.9)$$

The ξ^2 factors appearing in these equations are, in fact, absent in the standard spin-wave theories. However, Wang and Callen[12] have shown that they are introduced if spin-wave theory is suitably altered to treat the low-lying states accurately. And it is clear that these factors are required for quantum-mechanical consistency, at least in the case of spin $\frac{1}{2}$, for which the effective anisotropy constant $K\xi^2$ must vanish because $(S^z)^2$ is merely a constant.

The critical field H_c^a as given above also results from our analysis, but with additional quantum corrections, of the order of a few percent, arising from the lack of saturation of the sublattice magnetization in the ground state of the antiferromagnet. In addition, of course our analysis extends the critical field curve to nonzero temperatures.

To first order in K/zJ, the critical fields given above stand in the ratio

$$H_c^a : H_c^0 : H_c^J = \xi[1+(K/2zJ)(1+\xi^2)] : 1 : \times[\tfrac{1}{2}\xi(1+\xi)]^{1/2}[1-(K/4zJ)(5\xi^2+\xi-2)].$$

For fairly typical values of K and zJ, such as apply for instance to MnF_2,[16] $K/zJ \sim 0.01$, and the separation of the critical fields is of the order of $\pm 1\%$. In such cases the distinction among the critical fields would be difficult to observe experimentally, and our analysis of the stability boundary of the antiferromagnetic phase is operationally equivalent to a theory of the true phase transition. In $MnBr_2\cdot 4H_2O$, K/zJ is of the order of 13% and the three critical fields at the lower transition are appreciably separated. In fact, a hysteresis of this general magnitude is observed in upward and downward excursions through the transition.[4,5] In such cases the antiferromagnetic resonance experiments of Foner[17] are of special interest.

In a typical AFMR experiment an applied field is adjusted to bring the $\mathbf{k}=0$ spin-wave mode into reso-

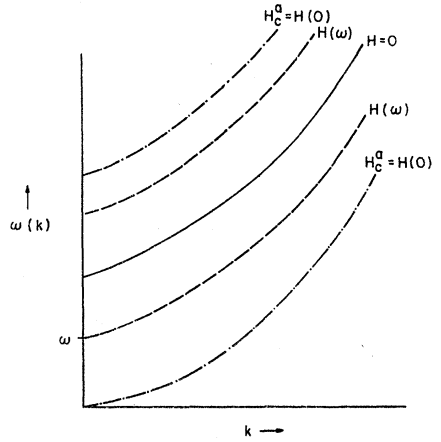

FIG. 4. Spin-wave spectrum of antiferromagnetic phase. For $H=0$ the two branches are degenerate. For an applied field $H(\omega)$ the branch which moves downward becomes degenerate at $\mathbf{k}=0$ with an applied AFMR signal frequency ω. For the applied field H_c^a the $\mathbf{k}=0$ mode becomes unstable.

[12] Yung-Li Wang and H. B. Callen, Phys. Chem. Solids (to be published).
[13] P. W. Anderson, Phys. Rev. **83**, 694 (1952).
[14] R. Kubo, Phys. Rev. **87**, 568 (1952).
[15] T. Oguchi, Phys. Rev. **117**, 117 (1960).
[16] See for example F. M. Johnson and A. H. Nethercot, Phys. Rev. **114**, 705 (1959); G. G. Low, A. Okazi, R. W. H. Stevenson, and K. C. Tuberfield, J. Appl. Phys. **35**, 998 (1964).
[17] S. Foner, Phys. Rev. **130**, 183 (1963).

nance with a specified signal frequency ω, rather than to reduce its frequency to zero. Such experiments have been carried out for instance by Foner[17] on single crystals of Cr_2O_3. The spin-wave spectrum of the antiferromagnet with an applied field is shown in Fig. 4. The field $H(\omega)$ required for AFMR at frequency ω is equal to H_c^a if $\omega=0$, and is less than H_c^a for $\omega\neq 0$. The loci of $H(\omega)$ are shown on the phase diagram in Fig. 5. Clearly, measurements of $H(\omega)$, extrapolated to $\omega=0$, give H_c^a even though the actual transition in a given material may occur at the lower field H_c^0. Thus the stability boundary of the antiferromagnetic phase can be measured by AFMR experiments. The temperature dependence of the $H(\omega)$ curves for arbitrary ω will be calculated in Sec. 7.

The salts $MnCl_2\cdot 4H_2O$ and $MnBr_2\cdot 4H_2O$ (Fig. 1) have been studied intensively. The Néel temperatures are of the order of 2°K and the critical fields H_c^0 [see Eq. (1.3)] for the flop-para transition are approximately 20 kOe. The anti-flop transition in $MnBr_2\cdot 4H_2O$ has been observed by Tsujikawa and Kanda[6] and by Bolger,[7] by the sudden shift in the optical absorption line at the transition. The anti-para transition in the same material was observed by Schelleng[4] by measurements of the specific-heat anomaly in crossing the transition curve. Using both single-crystal and powder specimens of the two salts, Henry[18] observed the change in magnetization with temperature for constant fields between 6 and 58 kOe; a bump appears in the magnetization curves as a function of temperature, locating both the anti-para and flop-para transitions.

Jacobs[19] also observed magnetization curves to study the anti-flop transition in MnF_2. This material has a Néel temperature of 68°K, so that the flop-para transition would be at unavailable field strengths, but the anti-flop transition is observed at 93 kOe at temperatures $\leqslant 20$°K.

If the anisotropy field is larger than, or comparable to, the exchange field, the spin-flop phase region contracts to zero area, or disappears. The resultant anti-para "metamagnetic" transition has been studied by Jacobs[20] in siderite ($FeCO_3$), for which the Néel temperature is 38°K. He again followed the magnetization as a function of field at constant temperature and found that for small temperatures the anti-para critical field is approximately 200 kOe. The same phenomenon has also been observed in hydrated $FeBr_2$ by Jacobs and Lawrence.[21] The Néel temperature is 11°K and the antipara critical field is approximately 31 kOe for low temperatures.

Because of the centrality of the spin-wave renormalization effect in the phase transition problem, we employ the method of two-time, temperature-dependent Green

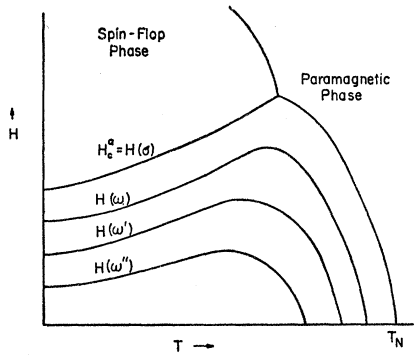

FIG. 5. Temperature dependence of the field for AFMR, for various signal frequencies.

functions[22] for arbitrary spin. Two decoupling approximations are explored: the random-phase approximation (RPA) as introduced by Tyablikov[23] and generalized by Tahir-Kheli and ter Haar,[24] and the Callen[25] decoupling approximation (CD). We shall find that at low temperatures CD agrees with spin-wave expansions for the sublattice magnetizations and the paramagnetic phases, and with the spin-wave expansions for both phase transition boundaries. Whereas RPA, like molecular field theory, gives a constant perpendicular susceptibility in the antiferromagnetic phase, CD predicts a decrease with temperature, qualitatively similar to that observed, for instance, in MnF_2.[26] However, neither approximation is adequate in the neighborhood of the Néel temperature.

In the ferromagnetic case the decoupling approximations recently have been investigated by Tahir-Kheli,[27] by an *ad hoc* determination of the optimum decoupling to obtain agreement with all available rigorous series-expansion results. He found that the optimum decoupling was the CD, but that an additional inhomogeneous term of the form suggested by the work of Wortis[28] is present. This inhomogeneous term is particularly large for $S=\frac{1}{2}$, but for other spin values it has significant values only in the vicinity of the Curie temperatures. We accordingly expect the CD results for the antiferromagnet to be satisfactory for $S\neq\frac{1}{2}$ and for temperatures comparable to, but not in the immediate neighborhood of, the Néel temperature.

The phase diagram has been previously studied extensively, using the Néel molecular-field model. Schelleng[4] gives an excellent review of these studies. The model is useful in indicating general qualitative be-

[18] W. Henry, Phys. Rev. **94**, 1146 (1954).
[19] I. S. Jacobs, J. Appl. Phys. Suppl. **32**, 1289 (1962).
[20] I. S. Jacobs, J. Appl. Phys. **34**, 1106 (1963).
[21] I. S. Jacobs and P. E. Lawrence, J. Appl. Phys. **35**, 996 (1964).
[22] N. N. Bogolyubov and S. V. Tyablikov, Dokl. Akad. Nauk SSSR **126**, 53 (1959) [English transl.: Soviet Phys.—Doklady **4**, 589 (1959)]. A good review article is given by D. N. Zubarev, Usp. Fiz. Nauk **71**, 71 (1960) [English transl.: Soviet Phys.—Usp. **3**, 320 (1960)].
[23] S. V. Tyablikov, Ukr. Nat. Zh. **11**, 287 (1961).
[24] R. A. Tahir-Kheli and D. ter Haar, Phys. Rev. **127**, 88 (1962).
[25] H. B. Callen, Phys. Rev. **130**, 890 (1963).
[26] J. W. Stout and M. Griffel, J. Chem. Phys. **18**, 1455 (1950).
[27] R. A. Tahir-Kheli, Phys. Rev. **132**, 689 (1963).
[28] M. Wortis, Ph.D. thesis, Harvard University, 1963 (unpublished).

havior, although quantitatively it is in serious disagreement with the rigorous results in the special regions where these are available.

The general problems here considered have received little theoretical attention. The spin-flop phase has been analyzed by Fu-Cho Pu[29] for the special case of spin $\frac{1}{2}$ and zero anisotropy, using a Green-function method. A standard spin-wave analysis of this phase has been carried out by Wang and Callen[12] for general spin and including anisotropy, but restricted, of course, to low temperature. Falk[30] has used a variational method valid at low temperatures for the case of zero anisotropy but general spin. Falk has also calculated the flop-para transition curve; using CD we find complete agreement with his result in the low-temperature region. The paramagnetic phase at low temperature is formally identical to a ferromagnet and is therefore described by standard spin-wave theory. At high temperatures many terms in the expansion of the susceptibility in powers of $1/T$ have been calculated and studied.[31] The antiferromagnetic phase for small fields has been studied most extensively. In the low-temperature spin-wave region, an excellent review article of previous treatments has been given by Nagamiya, Yosida, and Kubo.[32] The Green-function method for arbitrary temperature, but for spin $\frac{1}{2}$ only, has been applied by Ginsburg and Fain.[33] While writing up the results of our own investigation we have also received a preprint of a similar Green-function analysis of the antiferromagnetic phase by Hewson and ter Haar[34]; these authors, incidentally, treat the case of anisotropic exchange rather than uniaxial anisotropy, thereby avoiding the formal difficulty of decoupling.

2. GREEN-FUNCTION EQUATIONS: ANTIFERROMAGNETIC PHASE

For the model described in the second paragraph of the Introduction the Hamiltonian is

$$\mathcal{H}=\sum_{f,g} J_{fg}[\tfrac{1}{2}(f^+g^-+f^-g^+)+f^zg^z] -\mu H[\sum_f f^z+\sum_g g^z]-K[\sum_f (f^z)^2+\sum_g (g^z)^2]. \quad (2.1)$$

Here μS is the magnetic moment per ion, H is the external magnetic field (directed along the negative z axis), and f and g label the sites, respectively, of each of the two interpenetrating sublattices into which the lattice is assumed to be decomposable. Furthermore, for economy of notation, we denote the spin operator $S_f{}^z$ by f^z, and $S_f{}^\pm \equiv S_f{}^x \pm iS_f{}^y$ by $f^\pm$. The temperature-dependent Green function is defined by

$$\langle\langle A(t);B\rangle\rangle=\left\{\begin{array}{ll} -i\theta(t)\langle[A(t),B]\rangle & (t>0) \\ i\theta(t)\langle[A(t),B]\rangle & (t<0)\end{array}\right\}. \quad (2.2)$$

The function $\theta(t)$ is the unit step function (zero for negative argument and unity for positive argument), the single angular brackets denote an average with respect to the canonical density operator $\exp[-\beta\mathcal{H}]$, $(\beta=1/k_BT)$, and the square brackets denote the commutator. The Fourier transform of the Green function with respect to the time is denoted by $\langle\langle A;B\rangle\rangle$. The equation of motion satisfied by this function is

$$E\langle\langle A;B\rangle\rangle=(1/2\pi)\langle[A,B]\rangle+\langle\langle[A,\mathcal{H}];B\rangle\rangle. \quad (2.3)$$

Knowledge of $\langle\langle A;B\rangle\rangle$ suffices to determine the correlation function $\langle BA(t)\rangle$ in the usual fashion.[22]

We consider here the Green function $\langle\langle l^+;\tilde{\jmath}\rangle\rangle$ where, for convenience, we also introduce the notation

$$\tilde{\jmath}=e^{aj^z}j^-, \quad (2.4)$$

where l and j can be on either sublattice and a is a parameter introduced for the purpose described in Ref. 25. The equation of motion of the Green function is

$$(E-\mu H)\langle\langle l^+;\tilde{\jmath}\rangle\rangle=(1/2\pi)\langle[l^+,\tilde{\jmath}]\rangle+K\langle\langle l^+l^z+l^zl^+;\tilde{\jmath}\rangle\rangle +\sum_i J_{li}\langle\langle l^zi^+-l^+i^z;\tilde{\jmath}\rangle\rangle. \quad (2.5)$$

We adopt decoupling procedures analogous to those used previously in the study of the Heisenberg ferromagnet:

$$\langle\langle f^zg^+;\tilde{\jmath}\rangle\rangle\rightarrow\langle f^z\rangle\langle\langle g^+;\tilde{\jmath}\rangle\rangle+\alpha\langle g^z\rangle\langle f^-g^+\rangle\langle\langle f^+;\tilde{\jmath}\rangle\rangle, \quad (2.6)$$

$$\langle\langle g^zf^+;\tilde{\jmath}\rangle\rangle\rightarrow\langle g^z\rangle\langle\langle f^+;\tilde{\jmath}\rangle\rangle+\alpha\langle f^z\rangle\langle g^-f^+\rangle\langle\langle g^+;\tilde{\jmath}\rangle\rangle, \quad (2.7)$$

where the random-phase approximation[23] and the heuristic decoupling scheme proposed by Callen[25] are obtained by appropriate choice of α:

$$\begin{array}{lll}\alpha= & 0 & (\text{RPA}) \\ & =1/(2S^2) & (\text{CD}).\end{array} \quad (2.8)$$

As discussed in Ref. 25, at low temperatures CD represents an approximate treatment of the deviation of f^z from $+S$ and of g^z from $-S$, whereas at high temperatures it represents an approximate treatment of the deviations of f^z and g^z from zero. This consideration contributes the factor $\langle g^z\rangle/S$ and $\langle f^z\rangle/S$ to the second terms of Eqs. (2.6) and (2.7), respectively; the alternative choice of $-\langle f^z\rangle/S$ and $\langle g^z\rangle/S$, respectively, can be shown to lead to internal inconsistency of the theory, as will be discussed following Eq. (3.24). Furthermore, CD can be visualized as an application of Wick's[35] theorem to the boson-like creation and destruction

[29] Fu-Cho Pu, Doklady Akad. Nauk. SSSR **131**, 1244 (1960) [English transl.: Soviet Phys.—Doklady **5**, 128 (1960)].
[30] H. Falk, Phys. Rev. **135**, A1382 (1964).
[31] C. Domb and M. F. Sykes, Phys. Rev. **128**, 168 (1962).
[32] T. Nagamiya, K. Yosida, and R. Kubo, *Advances in Physics* (Francis & Taylor, Ltd., London, 1955), Vol. 4, p. 1.
[33] V. L. Ginsburg and V. M. Fain, Zh. Eksperim. i Teor. Fiz. **39**, 1323 (1960) [English transl.: Soviet Phys.—JETP **12**, 923 (1961)].
[34] A. C. Hewson and D. ter Haar, Clarendon Laboratory, Oxford, Great Britain, Ref. No. 121/63 (unpublished paper).
[35] G. C. Wick, Phys. Rev. **80**, 268 (1950).

operators

$$a^\dagger(\mathbf{k})=(2S)^{-1/2}\sum_l e^{i\mathbf{k}\cdot\mathbf{R}_l}l_l^-;$$

this consideration contributes the remaining factors to the second terms of Eqs. (2.6) and (2.7).

For the Green functions which appear in the anisotropy terms, we adopt a decoupling analogous to Eqs. (2.6) and (2.7).

$$\langle\langle f^+f^z+f^zf^+;\tilde{j}\rangle\rangle\rightarrow [2\langle f^z\rangle-\alpha\langle f^z\rangle(\langle f^+f^-\rangle+\langle f^-f^+\rangle)]\langle\langle f^+;\tilde{j}\rangle\rangle, \quad (2.9)$$

$$\langle\langle g^+g^z+g^zg^+;\tilde{j}\rangle\rangle\rightarrow [2\langle g^z\rangle-\alpha\langle g^z\rangle(\langle g^+g^-\rangle+\langle g^-g^+\rangle)]\langle\langle g^+;\tilde{j}\rangle\rangle. \quad (2.10)$$

The choice $\alpha=0$ (RPA) corresponds in this case to the substitution of $2K\langle f^z\rangle f^z$ for $K(f^z)^2$ in the Hamiltonian; this is a sort of semi-molecular-field approximation for the anisotropy energy. The choice $\alpha=1/(2S^2)$ is less clearly motivated for the anisotropy terms (2.9) than for the exchange terms (2.6). However, we note that the argument in terms of the application of Wick's theorem to the boson-like operators $a(\mathbf{k})$ and $a^\dagger(\mathbf{k})$ proceeds in the same fashion. Furthermore, it is reassuring to note that this decoupling satisfies a necessary identity for spin $\frac{1}{2}$; we then have $f^+f^z+f^zf^+=0$ so that the Green function (2.9) must vanish. The right-hand member of Eq. (2.9) becomes $2\langle f^z\rangle(1-\langle f^+f^-\rangle-\langle f^-f^+\rangle)$. However, $f^+f^-+f^-f^+=1$ for spin $\frac{1}{2}$, so that the right-hand member of Eq. (2.9) does indeed vanish identically. Finally, it can easily be shown that the decoupling does give the famous $l(l+1)/2$ power law for the effective anisotropy coefficient at low temperatures.[36]

The Green-function equations of motion now become

$$[E-\mu H+\langle g^z\rangle(zJ-\alpha\textstyle\sum_g J_{fg}\langle f^-g^+\rangle) -zJ\epsilon_f\langle f^z\rangle]\langle\langle f^+;\tilde{j}\rangle\rangle =[\theta_f(a)/2\pi]\delta_{fj}+\textstyle\sum_g J_{fg}\langle f^z\rangle \times(1-\alpha\langle g^-f^+\rangle)\langle\langle g^+;\tilde{j}\rangle\rangle \quad (2.11)$$

and

$$[E-\mu H+\langle f^z\rangle(zJ-\alpha\textstyle\sum_f J_{fg}\langle g^-f^+\rangle) -zJ\epsilon_g\langle g^z\rangle]\langle\langle g^+;\tilde{j}\rangle\rangle =[\theta_g(a)/2\pi]\delta_{gj}+\textstyle\sum_f J_{fg}\langle g^z\rangle \times(1-\alpha\langle f^-g^+\rangle)\langle\langle f^+;\tilde{j}\rangle\rangle, \quad (2.12)$$

where z is the number of nearest neighbors and J is the value of J_{fg} for the nearest-neighbor spins. Further

$$\epsilon_f=(2K/zJ)[1-\alpha\langle f^-f^+\rangle-\alpha\langle f^z\rangle], \quad (2.13)$$

$$\epsilon_g=(2K/zJ)[1-\alpha\langle g^-g^+\rangle-\alpha\langle g^z\rangle], \quad (2.14)$$

and, as in Ref. 25,

$$\theta_l(a)=\langle[l^+,\tilde{l}^-]\rangle =[S(S+1)(e^{-a}-1)+(e^{-a}+1)(d/da) -(e^{-a}-1)(d^2/da^2)]\langle e^{al^z}\rangle. \quad (2.15)$$

[36] C. Zener, Phys. Rev. **96**, 1335 (1954). See also a review article by J. H. Van Vleck, J. Phys. Rad. **20**, 124 (1959).

We further note that

$$\theta_l(0)=2\langle l^z\rangle. \quad (2.16)$$

3. FORMAL SOLUTION: ANTIFERROMAGNETIC PHASE

To diagonalize Eqs. (2.11) and (2.12), we introduce Fourier transforms:

$$G_{rr'}(\mathbf{k},a)=\sum_l\langle\langle l^+;\tilde{j}\rangle\rangle e^{-i\mathbf{k}\cdot\mathbf{R}_{lj}} \quad (3.1)$$

or inversely

$$\langle\langle l^+;\tilde{j}\rangle\rangle=-\frac{2}{N}\sum_{\mathbf{k}} G_{rr'}(\mathbf{k},a)e^{i\mathbf{k}\cdot\mathbf{R}_{lj}}. \quad (3.2)$$

Here $\mathbf{k}$ is a wave vector ranging over the first Brillouin zone of the magnetic lattice. The subscripts on $G(\mathbf{k},a)$ merely denote the sublattices to which the ions belong; r takes the values u (up), or d (down) according to the sublattice of l, and r' takes the values u, d, according to the sublattice of j. Hence G can have the four distinct subscripts (uu), (ud), (du), (dd). The Fourier transforms of the correlation functions carry similar subscripts, r again specifying the sublattice of l and r' the sublattice of j:

$$\psi_{rr'}(\mathbf{k},a)=\sum_l\langle\tilde{j}l^+\rangle e^{-\mathbf{k}\cdot\mathbf{R}_{lj}}. \quad (3.3)$$

The correlation function of nearest-neighbor spins plays a particularly important role, and we therefore find it convenient to define:

$$\psi_\delta=\langle f^-g^+\rangle \quad (g \text{ nearest neighbor of } f) \quad (3.4)$$

and we note that this correlation function has the same value for all nearest-neighbor pairs of f and g.

Finally, we define the transform of J_{fg}

$$J(\mathbf{k})\equiv zJ\gamma_{\mathbf{k}}=J\sum_{\boldsymbol{f}} e^{-i\mathbf{k}\cdot\mathbf{R}_{fg}}. \quad (3.5)$$

Multiplying Eq. (2.11) by $e^{-i\mathbf{k}\cdot\mathbf{R}_{fj}}$ and Eq. (2.12) by $e^{-i\mathbf{k}\cdot\mathbf{R}_{gi}}$ and summing over f and g, respectively, gives

$$[E-\mu H+zJ\langle g^z\rangle(1-\alpha\psi_\delta)-zJ\epsilon_f\langle f^z\rangle]G_{ur'}(\mathbf{k},a) =(1/2\pi)\theta_f(a)\Delta_{ur'}+J(\mathbf{k})\langle f^z\rangle(1-\alpha\psi_\delta^*)G_{dr'}(\mathbf{k},a), \quad (3.6)$$

$$[E-\mu H+zJ\langle f^z\rangle(1-\alpha\psi_\delta^*)-zJ\epsilon_g\langle g^z\rangle]G_{dr'}(\mathbf{k},a) =(1/2\pi)\theta_g(a)\Delta_{dr'}+J(\mathbf{k})\langle g^z\rangle(1-\alpha\psi_\delta)G_{ur'}(\mathbf{k},a), \quad (3.7)$$

where

$$\Delta_{rr'}\equiv 1, \quad r=r' \qquad \equiv 0, \quad r\neq r'. \quad (3.8)$$

Solving the two coupled equations for the Green func-

tions we find

$$G_{rr'}(\mathbf{k},a)=(1/2\pi)[E-h-b\nu(\mathbf{k},t)]^{-1}[E-h+b\nu(\mathbf{k},t)]^{-1}$$
$$\times\{\Delta_{ur}\Delta_{ur'}\theta_f(a)[E-\mu H+zJ\langle f^z\rangle(1-\alpha\psi_\delta^*)-zJ\epsilon_g\langle g^z\rangle]+\Delta_{dr}\Delta_{dr'}\theta_g(a)[E-\mu H+zJ\langle g^z\rangle(1-\alpha\psi_\delta)-zJ\epsilon_f\langle f^z\rangle]$$
$$+\Delta_{ur}\Delta_{dr'}\theta_g(a)J(\mathbf{k})\langle f^z\rangle(1-\alpha\psi_\delta^*)+\Delta_{dr}\Delta_{ur'}\theta_f(a)J(\mathbf{k})\langle g^z\rangle(1-\alpha\psi_\delta)\}, \quad (3.9)$$

where

$$h=\mu H-\tfrac{1}{2}zJ[\langle f^z\rangle(1-\alpha\psi_\delta^*-\epsilon_f)+\langle g^z\rangle(1-\alpha\psi_\delta-\epsilon_g)], \quad (3.10)$$

$$b=\tfrac{1}{2}zJ[\langle f^z\rangle(1-\alpha\psi_\delta^*+\epsilon_f)-\langle g^z\rangle(1-\alpha\psi_\delta+\epsilon_g)], \quad (3.11)$$

$$\nu(\mathbf{k},t)=(1-t^2\gamma_\mathbf{k}^2)^{1/2}, \quad (3.12)$$

and

$$t=(zJ/b)[-\langle f^z\rangle\langle g^z\rangle(1-\alpha\psi_\delta^*)(1-\alpha\psi_\delta)]^{1/2}. \quad (3.13)$$

The Fourier transform of the correlation function consequently is

$$\psi_{rr'}(\mathbf{k},a)=\Delta_{ur}\Delta_{ur'}\frac{\theta_f(a)}{2}\left[\phi_u(\mathbf{k})-\phi_l(\mathbf{k})-1+\frac{\phi_u(\mathbf{k})+\phi_l(\mathbf{k})+1}{\nu(\mathbf{k},t)}\right]$$
$$+\Delta_{dr}\Delta_{dr'}\frac{\theta_g(a)}{2}\left[\phi_u(\mathbf{k})-\phi_l(\mathbf{k})-1-\frac{\phi_u(\mathbf{k})+\phi_l(\mathbf{k})+1}{\nu(\mathbf{k},t)}\right]+\frac{zJ\gamma_\mathbf{k}}{2b\nu(\mathbf{k},t)}[\phi_u(\mathbf{k})+\phi_l(\mathbf{k})+1]$$
$$\times[\Delta_{ur}\Delta_{dr'}\theta_g(a)\langle f^z\rangle(1-a\psi_\delta^*)+\Delta_{dr}\Delta_{ur'}\theta_f(a)\langle g^z\rangle(1-\alpha\psi_\delta)], \quad (3.14)$$

where

$$\phi_{u,l}(\mathbf{k})=[\exp\beta E_{u,l}(\mathbf{k})-1]^{-1}. \quad (3.15)$$

The energies of the spin waves in the upper and lower branches are, as can be corroborated by comparison with conventional spin-wave theory,

$$E_{u,l}(\mathbf{k})=b\nu(\mathbf{k},t)\pm h, \quad (3.16)$$

where the positive sign is associated with the upper mode (u) and the negative sign with the lower mode (l). The Bose occupation numbers of these modes are $\phi_u(\mathbf{k})$ and $\phi_l(\mathbf{k})$. As in the ferromagnetic case it is convenient to introduce the Fourier transforms

$$\Phi_{u,l}(\mathbf{R})=(2/N)\textstyle\sum_\mathbf{k} e^{i\mathbf{k}\cdot\mathbf{R}}\phi_{u,l}(\mathbf{k}), \quad (3.17)$$

$$\Omega(\mathbf{R})=\frac{2}{N}\sum_\mathbf{k} e^{i\mathbf{k}\cdot\mathbf{R}}\frac{\phi_u(\mathbf{k})+\phi_l(\mathbf{k})+1}{2\nu(\mathbf{k},t)}. \quad (3.18)$$

The correlation functions of particular interest are

$$\langle e^{af_1^z}f_1^-f_2^+\rangle_{f_2=f_1+R}=\tfrac{1}{2}\theta_{f_2}(a)[\Phi_u(\mathbf{R})-\Phi_l(\mathbf{R})-\delta_{\mathbf{R},0}+2\Omega(\mathbf{R})], \quad (3.19)$$

$$\langle e^{ag_1^z}g_1^-g_2^+\rangle_{g_2=g_1+R}=\tfrac{1}{2}\theta_{g_2}(a)[\Phi_u(\mathbf{R})-\Phi_l(\mathbf{R})-\delta_{\mathbf{R},0}-2\Omega(\mathbf{R})], \quad (3.20)$$

$$\langle e^{af^z}f^-g^+\rangle_{g=f+\delta}=(1/b)zJ\theta_f(a)\langle g^z\rangle(1-\alpha\psi_\delta)(1/z)\textstyle\sum_{\delta'}\Omega(\boldsymbol{\delta}-\boldsymbol{\delta}'), \quad (3.21)$$

$$\langle e^{ag^z}g^-f^+\rangle_{f=g+\delta}=(1/b)zJ\theta_g(a)\langle f^z\rangle(1-\alpha\psi_\delta^*)(1/z)\textstyle\sum_{\delta'}\Omega(\boldsymbol{\delta}-\boldsymbol{\delta}'), \quad (3.22)$$

where the summation over $\boldsymbol{\delta}'$ extends over the z nearest-neighbor vectors. We also note that the function $\Omega(\mathbf{R})$, which appears frequently in the theory, can be related to the correlations of two spins a distance R apart, in each sublattice.

$$4\Omega(\mathbf{R})=\frac{\langle f_1^-f_2^+\rangle_{f_2=f_1+R}}{\langle f^z\rangle}-\frac{\langle g_1^-g_2^+\rangle_{g_2=g_1+R}}{\langle g^z\rangle}. \quad (3.23)$$

Equations (3.21) and (3.22) also evaluate ψ_δ, and with the aid of (2.16)

$$\psi_\delta=\psi_\delta^*=(1/b)2zJ\langle f^z\rangle\langle g^z\rangle(1-\alpha\psi_\delta)(1/z)\textstyle\sum_{\delta'}\Omega(\boldsymbol{\delta}-\boldsymbol{\delta}') \quad (3.24)$$

so that ψ_δ is real.

If a factor $-\alpha_f$ had been introduced into Eq. (2.6) in place of $\alpha\langle g^z\rangle$, and if α_g had replaced $\alpha\langle f^z\rangle$ in Eq. (2.7), Eq. (3.21) would contain the factor $(\langle g^z\rangle+\alpha_f\psi_\delta)$ whereas Eq. (3.22) would contain the factor $(\langle f^z\rangle-\alpha_g\psi_\delta^*)$. The consistency of these two equations would then demand $-\alpha_f\langle f^z\rangle=\alpha_g\langle g^z\rangle$. This was the basis for the form of decoupling assumed in Eqs. (2.6) and (2.7).

The three quantities determining the spin-wave energies (3.16) can now be written in terms of the sublattice magnetizations and the correlation functions.

$$b=\tfrac{1}{2}zJ(\langle f^z\rangle-\langle g^z\rangle)(1-\alpha\psi_\delta)+K(\langle f^z\rangle-\langle g^z\rangle)-\alpha K[(\langle f^z\rangle^2-\langle g^z\rangle^2)(\Phi_u(0)-\Phi_l(0))+2\Omega(0)(\langle f^z\rangle^2+\langle g^z\rangle^2)], \quad (3.25)$$

$$h=\mu H-\tfrac{1}{2}zJ(\langle f^z\rangle+\langle g^z\rangle)(1-\alpha\psi_\delta)+K(\langle f^z\rangle+\langle g^z\rangle)-\alpha K[(\langle f^z\rangle^2+\langle g^z\rangle^2)(\Phi_u(0)-\Phi_l(0))+2\Omega(0)(\langle f^z\rangle^2-\langle g^z\rangle^2)], \quad (3.26)$$

$$t=(zJ/b)(1-\alpha\psi_\delta)(-\langle f^z\rangle\langle g^z\rangle)^{1/2}. \quad (3.27)$$

In order to find the sublattice magnetization we set $R=0$ in Eq. (3.19) and note that it is identical in form to Eq. (42) of Ref. 25, whence

$$\langle f^z\rangle=\{[S-\Omega(0)-\tfrac{1}{2}(\Phi_u(0)-\Phi_l(0)-1)][1+\Omega(0)+\tfrac{1}{2}(\Phi_u(0)-\Phi_l(0)-1)]^{2S+1}$$
$$+[S+1+\Omega(0)+\tfrac{1}{2}(\Phi_u(0)-\Phi_l(0)-1)][\Omega(0)+\tfrac{1}{2}(\Phi_u(0)-\Phi_l(0)-1)]^{2S+1}\}$$
$$\times\{[1+\Omega(0)+\tfrac{1}{2}(\Phi_u(0)-\Phi_l(0)-1)]^{2S+1}-[\Omega(0)+\tfrac{1}{2}(\Phi_u(0)-\Phi_l(0)-1)]^{2S+1}\}^{-1}. \quad (3.28)$$

The expression for $\langle g^z\rangle$ is obtained by substituting the function

$$\tfrac{1}{2}[\Phi_u(0)-\Phi_l(0)-1]-\Omega(0)$$

for

$$\tfrac{1}{2}[\Phi_u(0)-\Phi_l(0)-1]+\Omega(0)$$

in the right-hand member of the above equation.

4. SUBLATTICE MAGNETIZATION AND SUSCEPTIBILITIES AT ZERO FIELD

For vanishing applied field the formalism simplifies greatly and we can easily evaluate the sublattice magnetization as a function of temperature. By obvious symmetry we have $\langle f^z\rangle=-\langle g^z\rangle$. This implies by Eq. (3.28) that $\Phi_u(0)=\Phi_l(0)$, and by Eqs. (3.15) and (3.16) in turn that $h=0$. In addition we find:

$$\psi_\delta=-2\langle f^z\rangle t(z^{-1})\textstyle\sum_{\delta'}\Omega(\boldsymbol{\delta}-\boldsymbol{\delta}'), \quad (4.1)$$

$$t^{-1}=1+\frac{2K}{zJ}\frac{1-2\alpha\langle f^z\rangle\Omega(0)}{1+2\alpha\langle f^z\rangle t(z^{-1})\sum_{\delta'}\Omega(\boldsymbol{\delta}-\boldsymbol{\delta}')}, \quad (4.2)$$

$$b=zJ\langle f^z\rangle[t^{-1}+2\alpha\langle f^z\rangle z^{-1}\textstyle\sum_{\delta'}\Omega(\boldsymbol{\delta}-\boldsymbol{\delta}')], \quad (4.3)$$

$$\Omega(\mathbf{R})=(2/N)\textstyle\sum_{\mathbf{k}}\exp(i\mathbf{k}\cdot\mathbf{R})(1-t^2\gamma_{\mathbf{k}}^2)^{-1/2}$$
$$\times\{[\exp\beta b(1-t^2\gamma_{\mathbf{k}}^2)^{1/2}-1]^{-1}+\tfrac{1}{2}\}, \quad (4.4)$$

and

$$\langle f^z\rangle=[(S+\tfrac{1}{2}-\Omega(0))(\Omega(0)+\tfrac{1}{2})^{2S+1}$$
$$+(S+\tfrac{1}{2}+\Omega(0))(\Omega(0)-\tfrac{1}{2})^{2S+1}]$$
$$\times[(\Omega(0)+\tfrac{1}{2})^{2S+1}-(\Omega(0)-\tfrac{1}{2})^{2S+1}]^{-1}. \quad (4.5)$$

We further recall that, if a is the lattice constant

$$\gamma_{\mathbf{k}}=\tfrac{1}{3}(\cos k_xa+\cos k_ya+\cos k_za) \quad \text{(sc)}, \quad (4.6)$$

$$\gamma_{\mathbf{k}}=\cos\tfrac{1}{2}k_xa\cos\tfrac{1}{2}k_ya\cos\tfrac{1}{2}k_za \quad \text{(bcc)}. \quad (4.7)$$

The perpendicular susceptibility is determined by the correlation functions through the well-known relation[37]

$$\chi^\perp=\beta\mu^2\sum_{i,j}\langle i^xj^x\rangle. \quad (4.8)$$

Expressing i^x, j^x in terms of $i^\pm$, $j^\pm$ and using Eq. (3.14) to evaluate the nonzero correlation functions, one obtains

$$\chi^\perp=\beta\mu^2N\langle f^z\rangle(1-t)\frac{\phi_u(0)+\phi_l(0)+1}{2\nu(0,t)}. \quad (4.9)$$

[37] Any standard textbook in statistical mechanics or in particular J. H. Van Vleck, *Theory of Electric and Magnetic Susceptibilities* (Clarendon Press, Oxford, 1932).

By straightforward differentiation, one finds that

$$\left[\frac{\partial}{\partial H}\Omega(0)\right]_{H=0}=0, \quad (4.10)$$

from which it follows that the parallel susceptibilities of the individual sublattices are equal, and each is half of the total parallel susceptibility:

$$\chi_f{}^\parallel=\chi_g{}^\parallel=\tfrac{1}{2}\chi^\parallel, \quad (4.11)$$

where

$$\chi_f{}^\parallel=\tfrac{1}{2}N\mu\left[\frac{\partial}{\partial H}\langle f^z\rangle\right]_{H=0} \quad (4.12)$$

and similarly for the definition of $\chi_g{}^\parallel$.

If the anisotropy constant is negligible, the equations for the sublattice magnetizations and susceptibilities simplify further. Then $t=1$ and $\Omega(\mathbf{R})$ can be evaluated [by Eq. (4.4)] in terms of the single parameter βb, thereby also determining $\langle f^z\rangle$ [through Eq. (4.5)] in terms of βb. Furthermore, we can rewrite Eq. (4.3) in the form

$$k_BT=\frac{zJ\langle f^2\rangle}{\beta b}\left[1+2\alpha\langle f^z\rangle\frac{1}{z}\sum_{\delta'}\Omega(\boldsymbol{\delta}-\boldsymbol{\delta}')\right] \quad (4.13)$$

so that k_BT is also known in terms of the parameter βb, and elimination of βb between these equations yields the sublattice magnetization as a function of temperature for all temperatures below the Néel point.

Similarly, the perpendicular susceptibility becomes, for zero anisotropy,

$$\chi^\perp=\tfrac{1}{2}\mu^2N\langle f^z\rangle/b$$
$$=\frac{\mu^2N}{2zJ}\left[1+2\alpha\langle f^z\rangle\frac{1}{z}\sum_{\delta'}\Omega(\boldsymbol{\delta}-\boldsymbol{\delta}')\right]^{-1}. \quad (4.14)$$

For $\alpha=0$ the perpendicular susceptibility is independent of temperature and is equal to the value given by molecular-field theory.[38]

The parallel susceptibility, for zero anisotropy, becomes

$$\chi_f{}^\parallel\Big/\left(\mu-\chi_f{}^\parallel\frac{b}{\langle f^z\rangle}\frac{2}{\mu N}\right)$$
$$=(\mu N/2)\beta I(\Omega)\frac{2}{N}\sum_{\mathbf{k}}\exp\beta b(1-\gamma_{\mathbf{k}}^2)^{1/2}$$
$$\times[\exp\beta b(1-\gamma_{\mathbf{k}}^2)^{1/2}-1]^{-2}, \quad (4.15)$$

[38] See Ref. 32.

TABLE I. Quantum correction constants and coefficients in low-temperature expansions of $\Omega(0)$ in the antiferromagnetic phase [Eq. (5.6)] and of $\Phi(0)$ in the paramagnetic phase [Eq. (9.11)]. [$\zeta(n)$ is the Riemann zeta function defined by $\zeta(n)=\sum_{p=1} p^{-n}$.]

	Simple cubic	Body-centered cubic
c'[a]	0.156	0.150
c[b]	0.097	0.073
a_0	$\frac{\zeta(2)}{\pi^2}3^{3/2}$	$\frac{\zeta(2)}{\pi^2}4$
a_1	$\frac{\zeta(4)}{\pi^2}6\times3^{3/2}$	$\frac{\zeta(4)}{\pi^2}24$
b_0	$\zeta(\frac{3}{2})(3/2\pi)^{3/2}$	$\frac{\zeta(\frac{3}{2})}{\pi^{3/2}}2^{1/2}$
b_1	$\zeta(\frac{5}{2})\frac{9}{8}(3/2\pi)^{3/2}$	$\frac{\zeta(\frac{5}{2})}{\pi^{3/2}}\frac{9}{8}2^{1/2}$

[a] $c'\equiv c'(1)$ [Eq. (5.4)].
[b] $c\equiv c_0-c'$ [Eq. (5.8)].

where

$$I(\Omega)=\frac{1-(2S+1)^2(\Omega^2(0)-\frac{1}{4})^{2S}}{[(\Omega(0)+\frac{1}{2})^{2S+1}-(\Omega(0)-\frac{1}{2})^{2S+1}]^2}. \quad (4.16)$$

We can use Eqs. (4.4), (4.5), and (4.16) to find $\chi_f{}^{\parallel}$ as a function of βb and, as in the analysis of the sublattice magnetization, the parameter βb can be eliminated by Eq. (4.13), yielding the parallel susceptibility for all temperatures below the Néel point.

For arbitrary temperatures, all the above calculations must be carried out by a computer, for specific numerical values of the parameters. In specific temperature regions, however, we can obtain general results by series expansion.

5. LOW-TEMPERATURE REGION

In order to evaluate explicitly the sublattice magnetization for $H=0$, at low temperatures, we first expand $\langle f^z\rangle$ in powers of the small quantity $\Omega(0)-\frac{1}{2}$.

$$\langle f^z\rangle=S-(\Omega(0)-\tfrac{1}{2})+(2S+1)(\Omega(0)-\tfrac{1}{2})^{2S+1}+\cdots. \quad (5.1)$$

The function $\Omega(0)$ is then expanded in powers of the reduced temperature

$$\tau=k_BT/zJ. \quad (5.2)$$

The temperature-independent part of $\Omega(0)$ is

$$\Omega(0)=\tfrac{1}{2}[c'(t)+1], \quad (5.3)$$

where

$$c'(t)=(2/N)\textstyle\sum_{\mathbf{k}}(1-t^2\gamma_{\mathbf{k}}{}^2)^{-1/2}-1 \quad (5.4)$$

and the value[39] of c' for $t=1$ is listed in Table I. Thus at $T=0$,

$$\langle f^z\rangle=S(1-c'(t)/2S). \quad (5.5)$$

It is seen that the sublattice magnetization does not fully saturate even in the ground state. However, for the case of infinite anisotropy, $t=0$, $c'=0$, and the spins are completely aligned.

The effect of anisotropy on the spin-wave energy spectrum for $H=0$ can be seen by referring to Fig. 4. If no anisotropy were present, the spin-wave energy would be a linear function of k for small k, vanishing at $k=0$. However, finite anisotropy produces an energy gap at $k=0$, and also produces a deviation from linearity for small values of k. Eiselle and Keffer[40] have investigated the effect of anisotropy by a spin-wave analysis of the antiferromagnet at low temperatures. They found that there is an effective temperature T_{AE}, below which the anisotropy plays an important role in determining the sublattice magnetizations and susceptibilities. The temperature T_{AE} is a measure of the energy gap in the antiferromagnet, and from Eq. (1.8),

$$k_BT_{AE}=2S[K\xi^2(zJ+K\xi^2)]^{1/2}\approx\mu H_c{}^a.$$

Thus for any material for which $H_c{}^a$ is practically measurable ($H_c{}^a<10^5$ Oe), $T_{AE}\leq10°$K, whereas for a material of small $H_c{}^a$ such as $MnBr_2\cdot4H_2O$, $T_{AE}\approx0.6°$K. We shall accordingly take $K=0$ in the calculation of $\langle f^z\rangle$, $\chi^{\parallel}$, and $\chi^{\perp}$, so that our resultant temperature expansion becomes a formal one valid only for $T_{AE}\ll T\ll T_N$.

Expanding the exchange integral in powers of k, replacing sums by integrals in reciprocal space, and performing the integrations, we find:

$$\Omega(0)=\tfrac{1}{2}(c'+1)+a_0(zJ\tau/b)^2+a_1(zJ\tau/b)^4+O(zJ\tau/b)^6, \quad (5.6)$$

where $c'\equiv c'(1)$, a_0, and a_1 are constants which depend on the type of lattice and are listed in Table I. Performing a similar expansion for the function $\Omega(\boldsymbol{\delta}-\boldsymbol{\delta}')$, and using Eq. (4.3) we also find

$$b=zJ\langle f^z\rangle\{1+2\alpha\langle f^z\rangle[\tfrac{1}{2}c_0+a_0(zJ\tau/b)^2+O(zJ\tau/b)^6]\}, \quad (5.7)$$

where

$$c_0(t)=\frac{2}{N}\sum_{\mathbf{k}}\frac{t^2\gamma_{\mathbf{k}}{}^2}{(1-t^2\gamma_{\mathbf{k}}{}^2)^{1/2}}. \quad (5.8)$$

The constant $c_0\equiv c_0(1)$ can be written as $c_0=c'+c$, and the constant[39] c is listed in Table I. It should also be noted that the constant a_0 in (5.7) is identical to that appearing in (5.6) and that it is listed in Table I, whereas the term in $(zJ\tau/b)^4$ in (5.7) vanishes. Using Eq. (5.1) we now solve the set of equations self-consistently in powers of τ. The results are given for both RPA and CD

[39] Calculated by Anderson and Kubo. See Refs. 13 and 14.

[40] J. A. Eiselle and F. Keffer, Phys. Rev. **96**, 929 (1954).

(all terms of order c'^2 and c^2 have been dropped).

$S=\frac{1}{2}$, $\alpha=0$:

$$\langle f^z\rangle=b/zJ=\tfrac{1}{2}(1-c')-4a_0\tau^2 -16[a_1(1+2c')+2a_0^2(1+c')]\tau^4+O(\tau^6); \quad (5.9)$$

$S=\frac{1}{2}$, $\alpha=1/2S^2$:

$$b/zJ=\tfrac{1}{2}(1+c)-8a_0(c'+c)\tau^2+O(\tau^4), \quad (5.10)$$

$$\langle f^z\rangle=\tfrac{1}{2}(1-c')-4a_0[1-2(c'+c)]\tau^2-16[a_1(1-2c'+4c) -2a_0^2(1-7c'-8c)]\tau^4+O(\tau^6); \quad (5.11)$$

$S>\frac{1}{2}$, $\alpha=0$:

$$\langle f^z\rangle=b/zJ=S(1-(c'/2S))-a_0(1+(c'/S))\tau^2/S^2 -[a_1(1+(2c'/S))+2a_0^2(1+(5c'/2S))/S -(2S+1)^2a_0^{2S}(c'/2)(\tau/S)^{4(S-1)}]\tau^4/S^4+O(\tau^6); \quad (5.12)$$

$S>\frac{1}{2}$, $\alpha=1/2S^2$:

$$b/zJ=S(1+(c/2S))-a_0(c+2c')\tau^2/S^3+O(\tau^4), \quad (5.13)$$

$$\langle f^z\rangle=S(1-(c'/2S))-a_0(1-(c/S))\tau^2/S^2 -[a_1(1-(2c/S))+2a_0^2(c+2c')/S^2 -(2S+1)^2a_0^{2S}(c'/2)(\tau/S)^{4(S-1)}]\tau^4/S^4+O(\tau^6). \quad (5.14)$$

For comparison, the spin-wave result given by Oguchi[15] is

$$\langle f^z\rangle=S(1-(c'/2S))-a_0(1-(c/S))\tau^2/S^2 -a_1(1-(2c/S))\tau^4/S^4+O(\tau^6). \quad (5.15)$$

It is seen that both RPA and CD give the same result as spin-wave theory for the temperature-independent term in the sublattice magnetization. For $S>\frac{1}{2}$ the principal part of the τ^2 term agrees with spin-wave theory for both RPA and CD, but the small correction of order c agrees only in the CD approximation. In the τ^4 terms, both RPA and CD give spurious contributions proportional to a_0^2; these terms arise from the renormalization of the energy in the Green-function analysis, and in CD they are an order of magnitude smaller than in RPA. The coefficient of the a_1 part of the τ^4 term agrees only in CD. For $S=\frac{1}{2}$, the temperature-independent terms all agree, as well as the principal part of the τ^2 term, but now the correction of order c disagrees with spin-wave theory in both RPA and CD.

Using the previous results we can evaluate the perpendicular susceptibility from Eq. (4.14). The results are

$S\geq\frac{1}{2}$, $\alpha=0$:

$$\chi^\perp=\mu^2N/2zJ; \quad (5.16)$$

$S\geq\frac{1}{2}$, $\alpha=1/2S^2$:

$$\chi^\perp=\frac{\mu^2N}{2zJ}\left\{1-\frac{c+c'}{2S}-a_0\left[1-\frac{5c+4c'}{2S}\right]\frac{\tau^2}{S^3}+O(\tau^4)\right\}. \quad (5.17)$$

The spin-wave result of Oguchi is

$$\chi^\perp=\frac{\mu^2N}{2zJ}\left\{1-\frac{c+c'}{2S}-a_0\left(1-\frac{c}{S}\right)\frac{\tau^2}{S^3}+O(\tau^4)\right\}. \quad (5.18)$$

The temperature-independent term of the CD result agrees with spin-wave theory, whereas the RPA result lacks the quantum corrections and is identical with the molecular-field result.[38] The τ^2 term in CD deviates from spin-wave theory by a correction of order c, whereas RPA lacks all temperature-dependent terms.

To calculate the parallel susceptibility we first find from Eq. (3.17) that

$$\frac{1}{2}\left[\frac{\partial}{\partial H}(\Phi_u(0)-\Phi_l(0))\right]_{H=0} =-\left[\mu-\chi_f^{\parallel}\frac{b}{\langle f^z\rangle}\frac{2}{\mu N}\right](1/b)[2a_0(zJ\tau/b)^2 +4a_1(zJ\tau/b)^4+O(zJ\tau/b)^6]. \quad (5.19)$$

Using this result and Eqs. (3.28), and (5.9)–(5.14), we again solve self-consistently for the parallel susceptibility. The results are, to order τ^2

$S=\frac{1}{2}$, $\alpha=0$:

$$\chi^\parallel=2\chi_f^\parallel=(\mu^2N/zJ)[16a_0(1+c')\tau^2+O(\tau^4)]; \quad (5.20)$$

$S=\frac{1}{2}$, $\alpha=1/2S^2$:

$$\chi^\parallel=2\chi_f^\parallel=(\mu^2N/zJ)[16a_0(1-3c-2c')\tau^2+O(\tau^4)]; \quad (5.21)$$

$S>\frac{1}{2}$, $\alpha=0$:

$$\chi^\parallel=2\chi_f^\parallel=(\mu^2N/zJS) \times[2a_0(1+(3c'/2S))\tau^2/S^2+O(\tau^4)]; \quad (5.22)$$

$S>\frac{1}{2}$, $\alpha=1/2S^2$:

$$\chi^\parallel=2\chi_f^\parallel=(\mu^2N/zJS) \times[2a_0(1-(3c/2S))\tau^2/S^2+O(\tau^4)]. \quad (5.23)$$

The spin-wave result of Oguchi for the parallel susceptibility is

$$\chi^\parallel=(\mu^2N/zJS)[2a_0(1-(3c/2S))\tau^2/S^2+O(\tau^4)]. \quad (5.24)$$

The principal part of the τ^2 agrees with spin-wave theory for both RPA and CD. The quantum correction to the τ^2 term is given correctly by CD and incorrectly by RPA for $S>\frac{1}{2}$, but is given incorrectly by both decouplings for $S=\frac{1}{2}$. Although we do not exhibit the τ^4 terms, no spurious terms in a_0^2 appear in either RPA or CD, and the CD result is correct for $S>\frac{1}{2}$ but incorrect in the quantum correction for $S=\frac{1}{2}$, whereas RPA gives an incorrect quantum correction for all S.

6. HIGH-TEMPERATURE REGION

We first determine the Néel temperature, at which the sublattice magnetizations vanish in zero external field.

Near the Néel temperature the exponentials in the distribution function $\phi_u(\mathbf{k})=\phi_l(\mathbf{k})$ can be expanded and it is seen that the function $[\Omega(0)]^{-1}$ is small. Hence from Eq. (4.5), the sublattice magnetization is given by

$$\langle f^z\rangle=\tfrac{1}{3}S(S+1)\left\{[\Omega(0)]^{-1}-[\Omega(0)]^{-3}\times\left[\frac{S(S+1)}{15}-\frac{1}{20}\right]+O(\Omega(0))^{-4}\right\}. \quad (6.1)$$

In addition, it is found that

$$\Omega(0)=zJ\tau F_t(-1)(1/b)+(b/zJ\tau 12)+O(b/zJ\tau)^3 \quad (6.2)$$

and

$$b=zJ\langle f^z\rangle\{t^{-1}+2\alpha\langle f^z\rangle[(zJ\tau/bt^2)(F_t(-1)-1)+(b/zJ\tau t^2 12)(F_t(2)-1)+O(b/zJ\tau)^3]\}, \quad (6.3)$$

where

$$F_t(n)=(2/N)\textstyle\sum_{\mathbf{k}}(1-t\gamma_{\mathbf{k}})^n. \quad (6.4)$$

The values of $F_t(n)$ for $n=1$, 2, and $t=1$ (zero anisotropy) are[41]

$$F_1(1)=1, \quad F_1(2)=(z+1)/z. \quad (6.5)$$

For $n=-1$ and $t=1$ the summation has been evaluated by Watson[42]; it has the values

$$F_1(-1)=1.51638 \text{ (sc)}; \ 1.39320 \text{ (bcc)}. \quad (6.6)$$

The Néel temperature is determined by the following limits. From (6.1) and (6.2)

$$\lim_{\langle f^z\rangle\to 0}\langle f^z\rangle=\frac{S(S+1)}{3}\frac{b}{zJ\tau_N F_t(-1)}, \quad (6.7)$$

whereas, for (6.3)

$$\lim_{\langle f^z\to 0}b=zJ\langle f^z\rangle\left[t^{-1}+2\alpha\langle f^z\rangle\frac{zJ\tau_N}{bt^2}[F_t(-1)-1]\right], \quad (6.8)$$

whence

$$\tau_N=\tau_0(t)\{t^{-1}+2\alpha\tau_0(t)t^{-2}[F_t(-1)-1]\}, \quad (6.9)$$

where

$$\tau_0(t)=S(S+1)/3F_t(-1) \quad (6.10)$$

and

$$t^{-1}=1+\frac{2K}{zJ}\frac{1-2\alpha[S(S+1)/3]}{1+2\alpha[F(-1)-1]\tau_0 t^{-1}}. \quad (6.11)$$

We note that the effect of the anisotropy is to increase the value of the Néel temperature, as might be expected. For $K=0$ and $\alpha=1/2S^2$ the Néel temperatures are identical with the Curie temperatures of a ferromagnet with the same $|J|$, as given in Ref. 25; similarly for $\alpha=0$ they are the same as those obtained by Tahir-Kheli and ter Haar.[24] High-temperature expansions by Rushbrooke and Wood[43] give an estimate of the relation between the Néel temperature and the Curie temperature of materials with equal $|J|$, in the form

$$\tau_N=\tau_c[1+0.63/zS(S+1)]. \quad (6.12)$$

Thus, for example, the difference between the Néel and Curie temperatures is about 5% for $S=1$ in the simple cubic structure, and decreases for increasing spin. Our result of $\tau_N=\tau_c$ is therefore reasonable. The absolute value of τ_c has been estimated by Rushbrooke and Wood, as

$$k_BT_c/J=z\tau_c=(5/192)(z-1)[11S(S+1)-1]. \quad (6.13)$$

Comparisons of the results of RPA and CD with these results have been given in Refs. 24 and 25, but for convenience we give τ_N in Table II.

To expand the sublattice magnetization near T_N we use Eqs. (6.1)–(6.3), finding that to first order in $1-(\tau/\tau_N)$, and for $K=0$,

$$\langle f^z\rangle^2=C_\alpha(1-(\tau/\tau_N)), \quad (6.14)$$

where

$$C_\alpha=\frac{\dfrac{\tau_0^2\tau_N F(-1)}{(2\tau_N-\tau_0)}}{\dfrac{1}{12}+\dfrac{(2S-1)(2S+3)}{60F(-1)}-\dfrac{2\alpha\tau_0^2F(-1)}{12z(2\tau_N-\tau_0)}} \quad (6.15)$$

and $F(-1)\equiv F_1(-1)$, $\tau_0\equiv\tau_0(1)$. Values for C_α for the simple cubic and body-centered cubic lattices, and for various spin values are given in Table III. Since the Néel temperature predicted by CD is higher than that

TABLE II. Reduced Néel temperature (k_BT_N/zJ) in the antiferromagnetic phase [Eq. (6.9), $t=1$] and reduced temperature [$\tau(H_c=0)$] in the paramagnetic phase [Eq. (9.19)] determined for cubic lattices and nearest neighbor interaction.

S	RPA	CD antiferromagnetic	CD paramagnetic
	Simple cubic		
$\frac{1}{2}$	0.17	0.22	0.11
1	0.44	0.54	0.34
$\frac{3}{2}$	0.82	0.98	0.67
2	1.32	1.54	1.01
$\frac{5}{2}$	1.92	2.23	1.61
3	2.64	3.03	2.24
	Body-centered cubic		
$\frac{1}{2}$	0.18	0.23	0.14
1	0.48	0.57	0.39
$\frac{3}{2}$	0.90	1.04	0.75
2	1.44	1.64	1.24
$\frac{5}{2}$	2.09	2.37	1.82
3	2.87	3.23	2.53

[41] Easily corroborated from definition of exchange integral, Eq. (3.5).

[42] G. N. Watson, Quart. J. Math. **10**, 266 (1939). See also M. Tikson, J. Res. Natl. Bur. Std. **50**, 177 (1953).

[43] G. S. Rushbrooke and P. J. Wood, Mol. Phys. **1**, 257 (1958).

for RPA, the effect of CD for a given temperature is to increase the value of the sublattice magnetization in comparison with RPA.

Since the quantity $\langle f^z\rangle/b$ determines the perpendicular susceptibility [see Eq. (4.14)], it is also found from the solutions of Eqs. (6.1)–(6.3) that to first order in $1-(\tau/\tau_N)$,

$$\chi^{\perp}=\frac{\mu^2N}{2}\frac{\langle f^z\rangle}{b}=\frac{\mu^2N}{2zJ}\frac{\tau_0}{\tau_N}\left[1+D_\alpha\left(1-\frac{\tau}{\tau_N}\right)\right], \quad (6.16)$$

where

$$D_\alpha=\frac{2\alpha(F(-1)-1)\tau_0^2}{2\tau_N-\tau_0}\times\frac{\frac{1}{12}+\frac{(2S-1)(2S+3)}{60F(-1)}-\frac{F(-1)}{12z(F(-1)-1)}}{\frac{1}{12}+\frac{(2S-1)(2S+3)}{60F(-1)}-\frac{2\alpha\tau_0^2F(-1)}{12z(2\tau_N-\tau_0)}} \quad (6.17)$$

and the values of D_α are listed in Table IV. It should be pointed out that in CD the value of the perpendicular susceptibility at the Néel temperature is smaller than that given by RPA; the ratio of the two values is τ_0/τ_N. The slope of $\chi^{\perp}$ at T_N, as given by CD, is nonzero and negative. A more detailed comparison of RPA and CD for the perpendicular susceptibility will be given in Sec. 10.

Finally, to evaluate the parallel susceptibility Eq. (3.17) can be used to obtain,

$$\frac{1}{2}\left[\frac{\partial}{\partial H}[\Phi_u(0)-\Phi_l(0)]\right]_{H=0}=-\left[\mu-\chi_J^{\parallel}\frac{b}{\langle f^z\rangle}\frac{2}{\mu N}\right]\frac{1}{zJ\tau}\times[(zJ\tau/b)^2F(-1)-\tfrac{1}{12}+O(b/zJ\tau)^2]. \quad (6.18)$$

Using the previous results we find that the parallel and perpendicular susceptibilities become equal at the Néel temperature,

$$\chi_{\tau_N}^{\parallel}=\chi_{\tau_N}^{\perp} \quad (6.19)$$

and that

$$\frac{\chi_{\tau_N}^{\parallel}-\chi_{\tau}^{\parallel}}{\chi_{\tau_N}^{\parallel}}=G_\alpha\left(1-\frac{\tau}{\tau_N}\right), \quad (6.20)$$

where

$$G_\alpha=\frac{\tau_0}{2\tau_N-\tau_0}\times\frac{\frac{1}{12}+\frac{(2S-1)(2S+3)}{60F(-1)}+\frac{2\alpha\tau_0F(-1)}{12z}}{\frac{1}{12}+\frac{(2S-1)(2S+3)}{60F(-1)}-\frac{2\alpha\tau_0^2F(-1)}{12z(2\tau_N-\tau_0)}}. \quad (6.21)$$

We note that for $\alpha=0$, $G_\alpha=1$, so that in RPA a plot of $\ln\chi^{\parallel}$ versus the temperature ratio T/T_N should have a slope of $+1$ at the Néel temperature. Values of G_α are given for the two lattice types and various spin values in Table IV.

TABLE III. Coefficients C_α in the temperature expansion of $\langle f^z\rangle^2$ near $T=T_N$ [Eq. (6.15)].

	Simple cubic		Body-centered cubic	
S	RPA	CD	RPA	CD
$\frac{1}{2}$	0.49	0.42	0.54	0.47
1	2.12	2.10	2.23	2.21
$\frac{3}{2}$	4.79	5.25	4.94	5.33
2	8.40	9.90	8.58	9.80
$\frac{5}{2}$	12.90	16.04	13.69	15.32
3	18.26	23.64	18.46	22.72

7. ANTIFERROMAGNETIC RESONANCE (AFMR)

As described in the Introduction, AFMR measures the field $H(\omega)$ required to reduce the energy of a $\mathbf{k}=0$ spin wave to a value $\hbar\omega$, determined by the imposed signal frequency. Extrapolation of the field $H(\omega)$ to $\omega=0$ determines the critical field for the anti-flop transition.

Such measurements have been carried out, for instance, by Foner[17] on Cr_2O_3. The crystal structure of this material permits the decomposition into two sublattices with the nearest neighbors of a spin on a given sublattice belonging only to the other sublattice. The anisotropy is uniaxial, with a small effective anisotropy field of 700 Oe and an exchange field of 2.45×10^6 Oe, corresponding to a Néel temperature of 308°K. Foner's measurements are represented in Fig. 6, where $H(\omega)$ curves are given as functions of T, for two values of ω.

For a given signal frequency ω, there exists a temperature $T_a(\omega)$ at which the field $H(\omega)$ vanishes. This temperature $T_a(\omega)$ is equal to T_N for $\omega=0$, but is less than T_N for nonzero frequencies. Referring to Fig. 4, it can be seen that the temperature $T_a(\omega)$ is such that, for $H=0$, the $\mathbf{k}=0$ spin-wave energy is renormalized down to $\hbar\omega$. At higher temperatures the $\mathbf{k}=0$ spin-wave energy lies below $\hbar\omega$, and a field must be applied to drive $E_u(0)$ *up* to $\hbar\omega$. The required field $H(\omega)$ then in-

TABLE IV. Coefficients in the temperature expansions of perpendicular (D_α) and parallel susceptibility (G_α), using CD, near $T=T_N$ [Eqs. (6.17) and (6.21)]. Here

$D_\alpha=-[d\ln\chi^{\perp}/d(T/T_N)]_{T=T_N}$ [see Eq. (6.16)];

for RPA, $D_\alpha=0$.

$G_\alpha=[d\ln\chi^{\parallel}/d(T/T_N)]_{T=T_N}$ [see Eq. (6.20)];

for RPA, $G_\alpha=1$.

	Simple cubic		Body-centered cubic	
S	D_α	G_α	D_α	G_α
$\frac{1}{2}$	0.11	0.74	0.11	0.76
1	0.13	0.86	0.12	0.88
$\frac{3}{2}$	0.14	0.96	0.12	0.96
2	0.15	1.03	0.13	1.02
$\frac{5}{2}$	0.16	1.10	0.13	1.06
3	0.16	1.14	0.13	1.10

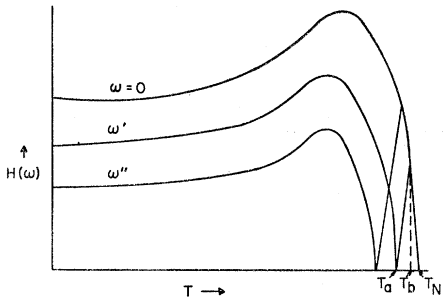

FIG. 6. Schematic of Foner's measurements on Cr_2O_3 ($\omega>0$) and anti-flop transition curve $H_c^a=H(\omega=0)$.

creases with temperature until the anti-para transition curve is crossed, at a temperature designated by $T_b(\omega)$ in Fig. 6.

In this section we restrict our analysis to signal frequencies ω which are appreciably greater than zero, permitting us to adopt a linear relation between the sublattice magnetizations and field.

$$\langle f^z\rangle=\langle f^z\rangle_{H=0}+2H\chi_f^{11}/\mu N\,, \tag{7.1}$$

$$\langle g^z\rangle=-\langle f^z\rangle_{H=0}+2H\chi_f^{11}/\mu N\,. \tag{7.2}$$

In this connection we note that at the stability boundary, corresponding to $\omega=0$, the differential susceptibility diverges and $\langle f^z\rangle$ is highly nonlinear in H, as is clear from Fig. 3(b). This case will be treated in the next section.

The quantities $\langle f^z\rangle$ and χ_f^{11} have been evaluated previously in the low- and high-temperature regions for zero anisotropy. Equation (3.16) determines the spin-wave energy, and for the lower branch at $k=0$,

$$E_l(0)=b(1-t^2)^{1/2}-h. \tag{7.3}$$

Equations (7.1), (7.2), and the previous results can now be used to find t as well as b and h. Setting $E_l(0)=\hbar\omega$ Eq. (7.3) can be solved for the external field $H(\omega)$. In the low-temperature region, and to order τ^2,

$$\mu H(\omega)=\mu H_c^a(T=0)[1+a_0(\tau^2/S^3)] -\hbar\omega[1+2a_0(\tau^2/S^3)] \quad (\tau\ll\tau_a), \tag{7.4}$$

where a_0 is the constant introduced in Eq. (5.6), and given in Table I, and where $H_c^a(T=0)$ depends on the choice of α as follows:

For $\alpha=0$,

$$\mu H_c^a(T=0)=zJS\left(1-\frac{c'}{2S}\right)\left[\frac{2K}{zJ}\left(2+\frac{2K}{zJ}\right)\right]^{1/2} \tag{7.5}$$

and for $\alpha=1/2S^2$,

$$\mu H_c^a(T=0)=zJS\left(1+\frac{c}{2S}\right) \times\left\{\frac{2K}{zJ}\left(1-\frac{1}{2S}\right)\left[2+\frac{2K}{zJ}\left(1-\frac{1}{2S}\right)\right]\right\}^{1/2}. \tag{7.6}$$

The effect of the anisotropy on the small constants c and c' has been neglected. Furthermore, corrections of order c have been neglected in the τ^2 terms in Eq. (7.4). As might be expected, $H_c^a(T=0)$ vanishes for $S=\frac{1}{2}$ in CD but not RPA.

The quantity $H_c^a(T=0)$ is identified as the critical field at zero temperature by letting $T=\omega=0$ in (7.4). We have accordingly designated this coefficient as $H_c^a(T=0)$. However, it should be recalled that the analysis required to compute H_c^a generally must take cognizance of the nonlinearity of the magnetization for fields near H_c^a, whereas Eq. (7.4) is based on an assumption of linearity. Nevertheless, the results given for $H_c^a(T=0)$ are correct, as will be corroborated in the next section, and the justification lies in the fact that the susceptibilities, linear or nonlinear, vanish at $T=0$.

To investigate the high-temperature behavior, the temperatures $\tau_a\equiv\tau_a(\omega)$ and $\tau_b\equiv\tau_b(\omega)$ must first be determined. τ_a is easily found by requiring $H(\omega)=0$, setting $E_l(0)=\hbar\omega$ in (7.3), and using the results of Sec. 6.

For $\alpha=0$,

$$1-\frac{\tau_a}{\tau_N}=(\hbar\omega/zJ)^2\Big/C_{\alpha=0}\frac{2K}{zJ}\left(2+2\frac{K}{zJ}\right) \tag{7.7}$$

and for $\alpha=1/2S^2$,

$$1-\frac{\tau_a}{\tau_N}=\left(\frac{\hbar\omega}{zJ}\right)^2\Big/C_{\alpha=1/2S^2}\frac{\tau_N}{\tau_0}\frac{(2S-1)}{3S}\frac{2K}{zJ} \times\left(2+2\frac{K}{zJ}\frac{(2S-1)}{3S}\frac{\tau_0}{\tau_N}\right), \tag{7.8}$$

where C_α, τ_0, and τ_N have been given in Sec. 6.

At the temperature τ_b, the field required to drive the upper spin-wave energy to $\hbar\omega$ reduces the lower one to zero. Since the two branches are symmetric around their value for $H=0$, it follows that at $\tau=\tau_b$, $E_{H=0}(0)=\hbar\omega/2$. This criterion enables us to find τ_b in terms of τ_a and τ_N:

$$\tau_b=\tfrac{3}{4}\tau_N+\tfrac{1}{4}\tau_a. \tag{7.9}$$

As in the low-temperature case, the required field $H(\omega)$ can be found from Eq. (7.3). Using Eqs. (7.7) and (7.8), a temperature expansion of $H(\omega)$ to first order in $\tau_a-\tau$ can be put in the convenient form:

$$\mu H(\omega)=\frac{\hbar\omega}{1+G_\alpha(1-(\tau_a/\tau_N))}\frac{\tau_a-\tau}{\tau_N-\tau_a}, \tag{7.10}$$

where G_α is the constant appearing in Eq. (6.20) and is listed in Table IV.

In the temperature range $T_a<T<T_b$, $H(\omega)$ is simply the negative of Eq. (7.10). It should be pointed out that the magnitude of the slope of $H(\omega)$ is large but finite, with negative sign for $\tau=\tau_a^-$ and positive sign for $\tau=\tau_a^+$.

The results of the theory are in qualitative agreement

with experiment. In the low-temperature region both theory and experiment indicate that the slope of the H-T curve is positive. In the vicinity of τ_a, the experiments of Foner indicate a large negative slope for $\tau<\tau_a$ and a large positive slope for $\tau>\tau_a$, again in agreement with theory.

A more quantitative comparison with experiment can be made by using Foner's experimental results on Cr_2O_3. Although the crystal structure of Cr_2O_3 is fairly complex, the magnetic lattice can be reasonably approximated by a body-centered cubic one. Measurements indicate that the magnetic ions have an effective spin $S=\frac{3}{2}$. The exchange integral can be evaluated by using Eq. (6.9) for T_N (with $t=1$) and equating it to the experimental Néel temperature of 308°K. The theoretical value of $H(\omega)$ at $T=0$, [given by Eqs. (7.4)–(7.6)], can be equated with the experimental value of 47 kOe corresponding to an AFMR frequency of 36 kMc/sec, thereby evaluating K. The comparisons between theory and experiment are given in Table V. The theory predicts an increase in $H(\omega)$ with temperature, with a slope which is virtually zero (to two significant figures) between $T=0$°K and $T=50$°K; this agrees with the experimental observations. Comparison of the temperatures $T_a(\omega)$ indicates that the results of CD are in much closer agreement with experiment than those given by RPA. Although not tabulated, the slope of the H-T curves at $T=T_a(\omega)$ also favors CD rather than RPA.

TABLE V. Comparison of theory and experiment. AFMR of Cr_2O_3 from Foner's (Ref. 17) measurements. J and K determined by $T_N=308$°K and the field for resonance at $T=0$, $\omega/2\pi=36$ kMc/sec. These values are starred in the table.

	Experiment	RPA	CD
For $\omega/2\pi=36$ kMc/sec:			
$H(\omega)$ at $T=0$	47 kOe*	47 kOe*	47 kOe*
$dH(\omega)/dT$ at $T=0$	0	0	0
T_a	304°K	301°K	305°K
For $\omega/2\pi=70.6$ kMc/sec:			
$H(\omega)$ at $T=0$	34 kOe	34 kOe	34 kOe
$dH(\omega)/dT$ at $T=0$	0	0	0
T_a	300°K	286°K	300°K

8. THE ANTI-FLOP TRANSITION BOUNDARY

As was indicated in the Introduction, the critical field for the anti-flop transition boundary is obtained by allowing the external field to increase until the $k=0$ value of the lower spin-wave energy branch, $E_l(0)$, vanishes, as illustrated in Fig. 4. On referring to Eq. (7.3) it is seen that the critical field is determined by the condition

$$h=b(1-t^2)^{1/2}. \tag{8.1}$$

Using expansions similar to those of Sec. 5 and Eq. (8.1), it is straightforward to determine the values at $T=0$ of the functions $\Phi_u(0)$, $\Phi_l(0)$, and $\Omega(0)$:

$$\Phi_u(0)=\Phi_l(0) \quad (T=0) \tag{8.2}$$

and

$$\Omega(0)=\tfrac{1}{2}(c'+1) \quad (T=0), \tag{8.3}$$

where again the effect of the anisotropy on the small quantity c' has been neglected. The sublattice magnetizations $\langle f^z\rangle_{T=0}$ and $\langle g^z\rangle_{T=0}$ can be found from Eqs. (8.2), (8.3), and (5.1).

$$\langle f^z\rangle=-\langle g^z\rangle=S(1-(c'/2S)). \tag{8.4}$$

These results are identical with those given in Eqs. (7.1) and (7.2) at $T=0$, since the susceptibility vanishes at zero temperature. Consequently, the zero-temperature value of the critical field calculated in the previous section is correct.

The situation becomes more complex, however, for the temperature-dependent terms. The assumption of a linear relation between the magnetization and external field, which was made in Sec. 7, is no longer valid. As indicated in Fig. 3(b), the susceptibility dM/dH becomes infinite (for $T\neq 0$) as point B is approached. The low-temperature expansions of Sec. 5 must also be carried out here, but any attempt to linearize the spin-wave energies $E_u(\mathbf{k})$ and $E_l(\mathbf{k})$ as functions of $\mathbf{k}$ results in a divergence of the integrals over $\mathbf{k}$ space. Hence the exchange integral must be expanded exactly for small values of $\mathbf{k}$,

$$(1-t^2\gamma_{\mathbf{k}}^2)^{1/2}=(1-t^2)^{1/2}+\tfrac{1}{2}t^2(1-t^2)^{-1/2}(1-\gamma_{\mathbf{k}}^2)+\cdots. \tag{8.5}$$

The distribution functions $\Phi_u(0)$ and $\Phi_l(0)$ can then be put in the following form:

$$\Phi_u(0)=\sum_{n=1}^{\infty}\exp[-2\beta bn(1-t^2)^{1/2}]\times P\left(\frac{zJ\tau(1-t^2)^{1/2}}{bnt^2}\right), \tag{8.6}$$

$$\Phi_l(0)=\sum_{n=1}^{\infty}P\left(\frac{zJ\tau(1-t^2)^{1/2}}{bnt^2}\right), \tag{8.7}$$

where

$$P(a)=\frac{2}{N}\sum_{\mathbf{k}}\exp\frac{a}{2}(1-\gamma_{\mathbf{k}}^2). \tag{8.8}$$

When the summation in Eq. (8.8) is replaced by an integral over $\mathbf{k}$ space, it is evident that the leading term in the function $P(zJ\tau(1-t^2)^{1/2}/bnt^2)$ will be proportional to $[zJ\tau(1-t^2)^{1/2}/bnt^2]^{3/2}$. To obtain a power series expansion in τ for the sublattice magnetizations, the coefficient of P in Eq. (8.6) must vanish. That is, the number of thermal spin waves excited by the upper branch must be negligibly small. This requirement is satisfied by the inequality

$$k_BT<2b(1-t^2)^{1/2}, \tag{8.9}$$

since

$$b(1-t^2)^{1/2}=\mu H_c{}^a=k_BT_{AE} \quad (T=0) \tag{8.10}$$

and T_{AE} is the characteristic temperature discussed in Sec. 5. The low-temperature expansions are valid in the temperature range $0<T<2T_{AE}$. This is an extremely restrictive range; for instance, $H_c^0(T=0)=60$ kOe in Cr_2O_3, and $T_{AE}\approx 10°K$. In this temperature range the formal expression for the critical field H_c^a would lead to a power series in the reduced temperature, $\tau^{3/2}$, $\tau^{5/2}$, etc., but this is of academic interest only. Furthermore, the experimental data are for $H(\omega)<H_c^0$ and even in this case $dH(\omega)/dT$ is approximately zero for $T<50°K$. Consequently we shall not carry out these calculations.

Both the CD and RPA treatments of the anti-flop transitions are inadequate in the neighborhood of the Néel temperature, as we shall now demonstrate. The temperature behavior of the critical field near the Néel temperature is determined by using Eq. (8.1) and expanding the functions $\Phi_u(0)$, $\Phi_l(0)$, and $\Omega(R)$ as in Sec. 6.

$$\tfrac{1}{2}[\Phi_u(0)-\Phi_l(0)] = -(1/bl^2)zJ\tau F(-1)(1-l^2)^{1/2}+O(b/zJ\tau), \quad (8.11)$$

$$z^{-1}\textstyle\sum_{\delta'}\Omega(\delta-\delta') = (1/bl^2)zJ\tau[F(-1)-1]+O(b/zJ\tau), \quad (8.12)$$

$$\Omega(0)=(1/bl^2)zJ\tau F(-1)+O(b/zJ\tau). \quad (8.13)$$

Expanding Eq. (3.28) in powers of $\{\frac{1}{2}[\Phi_u(0)-\Phi_l(0)-1]+\Omega(0)\}^{-1}$ for $\langle f^z\rangle$ and similarly for $\langle g^z\rangle$, the sublattice magnetizations are

$$\langle f^z\rangle=\frac{\tau_0}{zJ\tau}\frac{bl^2}{1-(1-l^2)^{1/2}}+O\left(\frac{b}{zJ\tau}\right), \quad (8.14)$$

$$\langle g^z\rangle=-\frac{\tau_0}{zJ\tau}\frac{bl^2}{1+(1-l^2)^{1/2}}+O\left(\frac{b}{zJ\tau}\right), \quad (8.15)$$

where

$$\tau_0=S(S+1)/3F(-1). \quad (8.16)$$

Multiplying Eqs. (8.14) and (8.15), using (3.24) and (3.27), and taking the limit $\langle f^z\rangle\to 0$, $\langle g^z\rangle\to 0$, which corresponds to $H_c^a\to 0$ [see Eqs. (8.1), (3.25) and (3.26)], $\tau(H_c^a=0)$ is evaluated to be

$$\tau(H_c^a=0)=\tau_0[1+2\alpha\tau_0(F(-1)-1)]. \quad (8.17)$$

This result implies that the temperature required for the vanishing of the critical field is independent of the anisotropy constant. We would expect that this temperature should be the Néel temperature as calculated in Sec. 6, but for finite anisotropy it is not. Furthermore, if we add Eqs. (8.14) and (8.15) and use (3.25) for b, then (taking $\alpha=0$)

$$\tau(H_c^a=0)=\tau_0(1+(2K/zJ)). \quad (8.18)$$

However, for $\alpha=0$, $\tau(H_c^a=0)=\tau_0$ from Eq. (8.17) and hence Eqs. (8.14) and (8.15) are inconsistent unless the anisotropy constant K is zero. Similar inconsistencies obtain for the case of $\alpha=1/2S^2$. We must conclude that the decoupling procedure (RPA or CD) is inadequate for the treatment of the anisotropy in the vicinity of the Néel temperature.

9. PARAMAGNETIC PHASE

The analysis of the paramagnetic phase is formally identical to that carried out for the ferromagnet in Ref. 25, except that the sign of the exchange integral is changed. The Hamiltonian is

$$\mathcal{H}=\tfrac{1}{2}\textstyle\sum_{f,g}J_{fg}(f^+g^-+f^zg^z) -\mu H\sum_f f^z-K\sum_f(f^z)^2, \quad (9.1)$$

where the factor $\frac{1}{2}$ is put before the exchange terms for consistency with the definition of the exchange integral used in the antiferromagnetic phase (our J is thus twice that of Ref. 25). The Green functions are decoupled as in Eq. (2.9) and Ref. 25. The Fourier transforms of the Green function, correlation function, and exchange integral are defined as in Eqs. (3.1), (3.3), and (3.5), except that now the subscripts r, r' are superfluous. N replaces $N/2$, and the Brillouin zone is now twice as large, containing only one rather than two spin-wave branches. Noting that $\psi_\delta=\psi_\delta{}^*$, the Green function equation of motion is given by

$$[E-E(\mathbf{k})]G(\mathbf{k},a)=\theta_f(a)/2\pi, \quad (9.2)$$

where

$$E(\mathbf{k})=\mu H-zJ\langle f^z\rangle(1-\alpha\psi_\delta)(1-\gamma_\mathbf{k})+zJ\epsilon_f\langle f^z\rangle \quad (9.3)$$

and ϵ_f is given by Eq. (2.13).

Again it is convenient to introduce the Fourier transform $\Phi(\mathbf{R})$ which is the analog of Eq. (3.17),

$$\Phi(\mathbf{R})=N^{-1}\textstyle\sum_\mathbf{k}e^{i\mathbf{k}\cdot\mathbf{R}}[e^{\beta E(\mathbf{k})}-1]^{-1}. \quad (9.4)$$

The correlation function may now be written as

$$\langle e^{a_jz}j^-l^+\rangle_{l=j+R}=\theta_j(a)\Phi(\mathbf{R}). \quad (9.5)$$

The correlation functions of particular interest are

$$\langle e^{a_jz}f^-f^+\rangle=\theta_f(a)\Phi(0), \quad (9.6)$$

$$\psi_\delta=\langle f^-g^+\rangle_{g=f+\delta}=2\langle f^z\rangle\Phi(\boldsymbol{\delta}), \quad (9.7)$$

and

$$E(\mathbf{k})=\mu H-zJ\langle f^z\rangle(1+\alpha\psi_\delta)(1-\gamma_\mathbf{k}) +2K\langle f^z\rangle[1-\alpha\langle f^z\rangle(2\Phi(0)+1)]. \quad (9.8)$$

Comparing Eqs. (9.6) and (3.19), it can be seen that the sublattice magnetization $\langle f^z\rangle$ can be obtained from Eq. (3.28) by replacing $\frac{1}{2}[\Phi_u(0)-\Phi_l(0)-1]+\Omega(0)$ by $\Phi(0)$.

It was demonstrated in the Introduction that the critical field for the para-anti or para-flop transitions can be found by requiring that $E(\mathbf{k})=0$ for values of $\mathbf{k}$ such that $-\gamma_\mathbf{k}=1$. The critical field H_c is then given by

$$\mu H_c=2zJ\langle f^z\rangle(1+\alpha\psi_\delta) -2K\langle f^z\rangle[1-\alpha\langle f^z\rangle(2\Phi(0)+1)]. \quad (9.9)$$

At the critical field $H=H_c$, the spin-wave energy $E(\mathbf{k})$ is

$$E(\mathbf{k})=zJ\langle f^z\rangle(1+\alpha\psi_\delta)(1+\gamma_k). \tag{9.10}$$

To explicitly evaluate the magnetization at low temperatures we use the analog of Eq. (5.1), expanding $\langle f^z\rangle$ in powers of $\Phi(0)$. The function $\Phi(0)$ can then be expanded in powers of the reduced temperature τ as defined by Eq. (5.2). It should be pointed out that the expansion of γ_k (sc) in powers of k must be carried out around $(\pi/a,\pi/a,\pi/a)$ rather than around (0,0,0) as in the antiferromagnetic or ferromagnetic case.

We find that

$$\Phi(0)=b_0[\tau/\langle f^z\rangle(1+\alpha\psi_\delta)]^{3/2} +b_1[\tau/\langle f^z\rangle(1+\alpha\psi_\delta)]^{5/2}+O(\tau)^{7/2} \tag{9.11}$$

and

$$\Phi(\boldsymbol{\delta})=-b_0[\tau/\langle f^z\rangle(1+\alpha\psi_\delta)]^{3/2} +\tfrac{1}{3}b_1[\tau/\langle f^z\rangle(1+\alpha\psi_\delta)]^{5/2}+O(\tau)^{7/2}, \tag{9.12}$$

where the constants b_0 and b_1 depend on the lattice structure but not on α; they are listed in Table I. Using Eqs. (9.7), (9.11), (9.12), and (5.1) with $\Phi(0)$ replacing $\Omega(0)-\frac{1}{2}$ we may solve the set of equations self-consistently in powers of τ. The results are

$$\langle f^z\rangle=S-b_0(\tau/S)^{3/2}-b_1(\tau/S)^{5/2}+\cdots, \tag{9.13}$$

$$1+\alpha\psi_\delta=1-2\alpha Sb_0(\tau/S)^{3/2} +2\alpha S(b_1/3)(\tau/S)^{5/2}+\cdots. \tag{9.14}$$

The magnetization is unaffected by the choice of α for terms to order $\tau^{5/2}$; furthermore, the magnetization to this order is the same as obtained in Ref. 25 for the zero-anisotropy ferromagnet with the same value of $|J|$. To this order the results agree with the spin-wave expansions of Dyson[8] for the ferromagnet; however, if the expansions were carried to any higher order, differences between these results and Dyson's would appear.

The critical field H_c can be found by using Eqs. (9.13) and (9.14) in Eq. (9.9).

$$\mu H_c=2zJS[1-(b_0/S)(\tau/S)^{3/2}(1+2\alpha S^2) -(b_1/S)(\tau/S)^{5/2}(1-\tfrac{2}{3}\alpha S^2)] -2KS[1-\alpha S-b_0(\tau/S)^{3/2} \times(2\alpha(S-1)+(1/S))]. \tag{9.15}$$

The effect of the anisotropy is to move the transition curve downward. However, for materials with high Néel temperatures and small anisotropy, such as Cr_2O_3, the effect of the anisotropy constant K can be neglected in comparison to the leading term of Eq. (9.15), which is the order of zJ.

It is instructive to find the temperature dependence of the spin-wave energy $E(0)$ at the critical field H_c. Using the previous results and Eq. (9.10) it is found that to order $\tau^{3/2}$,

$$E(0)=2zJS[1-(b_0/S)(1+2\alpha S^2)(\tau/S)^{3/2}+O(\tau)^{5/2}]. \tag{9.16}$$

Comparing this result with that for the ferromagnet[25] we note that the temperature dependence of the renormalization factor $\langle f^z\rangle(1+\alpha\psi_\delta)$ is $\tau^{3/2}$ rather than $\tau^{5/2}$. Furthermore, the choice of α makes a significant difference in the coefficient of the temperature terms in the expression for the critical field. The coefficient of $(\tau/S)^{3/2}$ is $2b_0/S$ in CD while it is b_0/S in RPA. In a paper employing a variational treatment using the Holstein-Primakoff variables, Falk[30] calculates the critical curve (zero anisotropy) in the low-temperature region. We find agreement with his results to order $\tau^{3/2}$ for the CD approximation. A more detailed discussion of the renormalization effects will be given in Sec. 10.

It would be expected that the critical field H_c should vanish at the Néel temperature. To find the temperature at which $H_c=0$, we expand the exponential in the distribution function $\Phi(\mathbf{R})$, and again the function $[\Phi(0)+\frac{1}{2}]^{-1}$ is small. Hence the analog of Eq. (6.1) can be used to determine the magnetization, with $\Phi(0)+\frac{1}{2}$ replacing $\Omega(0)$. The functions $\Phi(0)$ and $\Phi(\boldsymbol{\delta})$ are given by

$$\Phi(0)+\tfrac{1}{2}=\frac{\tau}{\langle f^z\rangle}\frac{F(-1)}{1+\alpha\psi_\delta}+\frac{\langle f^z\rangle}{12\tau}(1+\alpha\psi_\delta)+O\left(\frac{\langle f^z\rangle}{\tau}\right)^3, \tag{9.17}$$

$$\Phi(\boldsymbol{\delta})=-\frac{\tau}{\langle f^z\rangle}\frac{F(-1)-1}{1+\alpha\psi_\delta} +\frac{\langle f^z\rangle}{12\tau}(1+\alpha\psi_\delta)(F(2)-1)+O\left(\frac{\langle f^z\rangle}{\tau}\right)^3. \tag{9.18}$$

Taking the limit $\langle f^z\rangle\to 0$, the temperature at which $H_c=0$ [see Eq. (9.9)] is

$$\tau(H_c=0)=\tau_0[1-2\alpha\tau_0(F(-1)-1)], \tag{9.19}$$

where τ_0 was defined in Eq. (6.10), ($l=1$) and is equal to the Néel temperature in the RPA for zero anisotropy. Values of the temperature $\tau(H_c=0)$ for the two lattice types and various spin values are given in Table II.

It is interesting to compare the temperature given by Eq. (9.19) with that obtained in Sec. 8; that is, with the temperature at which the critical field of the antiferromagnetic phase vanishes [see Eq. (8.17)]. We would expect both of these values to be the Néel temperature as calculated in Sec. 4. We recall however, that in the lower transition the value of $\tau(H_c{}^a=0)$ was self-inconsistent. The expression for $\tau(H_c=0)$ in the upper phase transition is not self-inconsistent, but it is independent of the anisotropy, and hence it does not agree with the Néel temperature. Even in the absence of anisotropy, the temperatures $\tau(H_c{}^a=0)$ and $\tau(H_c=0)$ are identical only in RPA, and differ quite widely in CD, as can be seen in Table II. Hence we must again conclude that the decoupling procedures for the anisotropy are inadequate in the vicinity of the Néel temperature.

The magnetization $\langle f^z\rangle$ near $T(H_c=0)$ can be found from Eqs. (9.17) and (9.18) and to first order in

$1-[\tau/\tau(H_c=0)]$,

$$\langle f^z\rangle^2=L_\alpha[1-(\tau/\tau(H_c=0))], \tag{9.20}$$

where L_α is the same function of τ_0 and τ_N as was the similar quantity C_α given in Eq. (6.15). That is,

$$L_\alpha=\frac{\dfrac{\tau_0\tau(H_c=0)F(-1)}{2\tau(H_c=0)-\tau_0}}{\dfrac{1}{12}+\dfrac{(2S-1)(2S+3)}{60F(-1)}-\dfrac{2\alpha\tau_0^2F(-1)}{12z[2\tau(H_c=0)-\tau_0]}}. \tag{9.21}$$

In the vicinity of the temperature $\tau(H_c=0)$ the critical field can now be found using the previous results.

$$\mu H_c=2zJ\left\{L_\alpha\left[1-\frac{\tau}{\tau(H_c=0)}\right]\right\}^{1/2}\times\left[\frac{\tau(H_c=0)}{\tau_0}-\frac{K}{zJ}\left(1-2\alpha\frac{S(S+1)}{3}\right)\right]. \tag{9.22}$$

The critical field predicted by Eq. (9.22) vanishes and has an infinite slope for $\tau=\tau(H_c=0)$.

We have mentioned that the effect of the anisotropy on the para-flop transition curve is to move it downwards, while it moves the anti-flop curve upwards. It is interesting to determine the value of the anisotropy required for the two transition curves to meet at $T=0$. Using Eqs. (7.6) and (9.15) and recalling the definition of ξ in Eq. (1.7), we find that at $T=0$ (in CD) the spin-flop phase is absent if

$$K\xi^2/zJ\geq\tfrac{1}{3}. \tag{9.23}$$

Hence the anisotropy constant must be of the order of the exchange field. This condition is possible for materials with small Néel temperatures and large anisotropy fields. Under these conditions the antiferromagnetic phase would go over to the paramagnetic phase upon the application of an external field greater than the critical field given in Eq. (9.15). Siderite ($FeCO_3$) exhibits[20] such a metamagnetic transition (at approximately 200 kOe).

The paramagnetic susceptibility χ above the Néel temperature, where the spontaneous magnetization vanishes, can also be determined. Setting the anisotropy $K=0$ and $\langle f^z\rangle=\chi H/\mu^2N$, and retaining terms linear in H only, we find from Eq. (6.1) and the analogs of Eqs. (6.2) and (6.3) the following relations:

$$\frac{S(S+1)}{3}=\frac{zJ\tau\chi}{\mu^2N}\frac{1}{N}\times\sum_{\mathbf{k}}\left[1-\frac{zJ\chi}{\mu^2N}(1+\alpha\psi_\delta)(1-\gamma_{\mathbf{k}})\right]^{-1}, \tag{9.24}$$

$$1+\alpha\psi_\delta=\frac{zJ\tau\chi}{\mu^2N}\frac{1}{N}\times\sum_{\mathbf{k}}\gamma_{\mathbf{k}}\left[1-\frac{zJ\chi}{\mu^2N}(1+\alpha\psi_\delta)(1-\gamma_{\mathbf{k}})\right]^{-1}. \tag{9.25}$$

Expanding the summands in the above two equations, the susceptibility can be found as a power series in $1/\tau$. Using the relations given by Eq. (6.5) the result is

$$\chi=\frac{\mu^2N}{zJ}\frac{\tau_M}{\tau}\left[1-\frac{\tau_M}{\tau}+\left(\frac{\tau_M}{\tau}\right)^2\times\left(1-2\alpha\frac{S(S+1)}{3}\right)+O\left(\frac{1}{\tau^3}\right)\right], \tag{9.26}$$

where τ_M corresponds to the paramagnetic Néel temperature given by molecular field theory.

$$\tau_M=\tfrac{1}{3}S(S+1). \tag{9.27}$$

Equation (9.26) can be written approximately as

$$\chi=\frac{\mu^2N}{zJ}\frac{\tau_M}{\tau+\tau_M}. \tag{9.28}$$

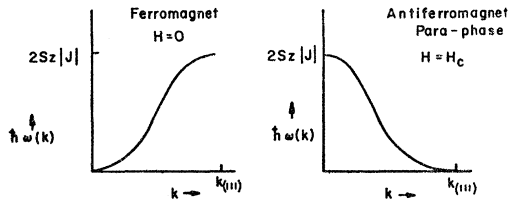

FIG. 7. Spin-wave spectra of ferromagnet at $H=0$, and antiferromagnet at the flop-para transition ($K=0$).

10. RESULTS AND DISCUSSION

The sublattice magnetizations, susceptibilities, and phase transition boundaries of both the antiferromagnetic and paramagnetic phases have been calculated, with results to be summarized and described below. Of particular physical interest is the temperature dependence of the flop-para transition curve, as it directly reflects the renormalization of the spin-wave modes in the paramagnetic phase [recall Eq. (1.3)]. The analysis of the paramagnetic phase at the transition is remarkably like the analysis of a ferromagnet at zero field. The change of sign of J inverts the spin-wave spectrum, and the critical field brings the mode at $\mathbf{k}=(\pi/a)(1,1,1)$ (sc) to zero frequency; a shift of origin of the Brillouin zone then makes the spectrum appear identical to that of a ferromagnet at zero field (see Fig. 7). It thereby might be expected that the flop-para transition curve would behave as $(1-\text{const}\tau^{5/2})$ at low temperatures, in agreement with the well known Dyson[8] result that the spin-wave energies are "renormalized by the energy ($\tau^{5/2}$)

rather than the magnetization ($\tau^{3/2}$)." This is not so, for the following reasons. Let us first recall that for zero anisotropy the renormalization factor is, according to Ref. 25 [also see Eq. (9.9)]

$$R=(\langle f^z\rangle/S)[1+(\psi_\delta/2S^2)], \tag{10.1}$$

where ψ_δ is the transverse correlation function of nearest neighbor spins

$$\psi_\delta=\langle f^- g^+\rangle_{g=f+\delta}. \tag{10.2}$$

If the thermally excited magnons are very long compared to the nearest-neighbor distance, as they are in the ferromagnet, ψ_δ is identical to the self-correlation function ψ_0 to leading order in a temperature expansion. This immediately relates the temperature dependence of ψ_δ to that of $\langle f^z\rangle$, and one obtains directly that if

$$\langle f^z\rangle/S=1-\zeta(\tfrac{3}{2})\tau'^{3/2}/S, \tag{10.3}$$

then

$$\psi_\delta\approx\psi_0=2S\zeta(\tfrac{3}{2})\tau'^{3/2}, \tag{10.4}$$

where τ' is an appropriate reduced temperature[8] and $\zeta(\frac{3}{2})$ is the Riemann zeta function. Then

$$R(\tau')=\left(1-\zeta(\tfrac{3}{2})\frac{\tau'^{3/2}}{S}+\cdots\right)\left(1+\zeta(\tfrac{3}{2})\frac{\tau'^{3/2}}{S}+\cdots\right)$$
$$=O(\tau^{5/2}) \tag{10.5}$$

This cancellation of the cross terms in Eq. (10.5) is the celebrated result of Dyson.

For the antiferromagnet at the flop-para transition the above considerations again apply, except that the thermally excited spin waves have precisely *opposite* phase for the nearest-neighbor ions, the thermal spin waves being centered at the edge of the Brillouin zone. Consequently, the correlation function has the magnitude given in Eq. (10.4) but *opposite sign.* Thus

$$R(\tau')=\left(1-\zeta(\tfrac{3}{2})\frac{\tau'^{3/2}}{S}+\cdots\right)\left(1-\zeta(\tfrac{3}{2})\frac{\tau'^{3/2}}{S}+\cdots\right)$$
$$=1-\frac{2}{S}\zeta(\tfrac{3}{2})\tau'^{3/2}+O(\tau'^{5/2}) \tag{10.6}$$

or, *the coefficient of $\tau'^{3/2}$ in the flop-para transition curve is twice that in the reduced magnetization of a ferromagnet with equal $|J|$.* The $\tau'^{5/2}$ terms in the flop-para transition boundaries have been given in Eq. (9.15).

Dyson has shown that the cancellation of the terms in a ferromagnet is related physically to the cancellation of kinematical corrections against dynamical-kinematical interference terms. The kinematical correction finds expression in the factor $\langle f^z\rangle/S$ in R, and the dynamical-kinematical term manifests itself in the correlation function ψ_δ. The cancellation of the cross terms in (10.5) is, then, the physical cancellation of kinematical and dynamical-kinematical terms. However, the effective spin-wave interaction in the antiferromagnet is repulsive rather than attractive as in the ferromagnet. *Thus the dynamical correction at the flop-para transition inverts the sign of the dynamical-kinematical interference and doubles the effect of the pure kinematical term $\langle f^z\rangle/S$, rather than cancelling it.*

Keffer and Loudon[10] have given another interesting heuristic interpretation for the renormalization of ferromagnetic spin waves by thermal excitation of others. They draw an analogy with waves on a liquid surface, and point out that a ripple superposed on a long wave senses only the local curvature of the surface produced by the latter. This curvature is analogous to the angle between neighboring spins, or to the energy. Hence a ripple is renormalized by the energy *if the thermal waves are all very long.* If the thermal waves are predominately short, the argument can be inverted, and the relevant measure of their effect is their total number (or, in the magnetic case, the magnetization). At the flop-para transition the thermal spin waves are very short and the renormalization does, indeed, occur by the magnetization ($\tau^{3/2}$).

Turning now to the lower transition, we examine the qualitative features of the renormalization of the antiferromagnetic spin-wave modes. At zero field the simple spin-wave modes[13–15] are doubly degenerate, with an energy gap related to the anisotropy [cf. Fig. 8(a)]. A field H then splits the degeneracy, moving the modes up and down by $\pm\mu H$. The renormalization then has two effects. Firstly, the curvature of the spectrum is flattened, decreasing the energy gap [Fig. 8(b)] from Δ to $R_1(\tau)\Delta$. Secondly, the effect of the field is reduced, the modes moving up and down by $\pm\mu H R_2(\tau)$. Thus $R_1(\tau)$ is the renormalization factor for the spin-wave energies at zero H, and $R_2(\tau)$ is the renormalization factor for the effective spin (or magnetic moment) carried by a spin wave. Both $R_1(\tau)$ and $R_2(\tau)$ decrease with increasing T. The field required to reduce the $\mathbf{k}=0$ mode to a given frequency ω is, then,

$$\mu H(\omega)=[R_1(\tau)/R_2(\tau)]\Delta-[\hbar\omega/R_2(\tau)]. \tag{10.7}$$

The competition of $R_1(\tau)$ and $R_2(\tau)$ is evidenced by the change in slope of the $H(\omega)$ versus T curves (Fig. 9), the

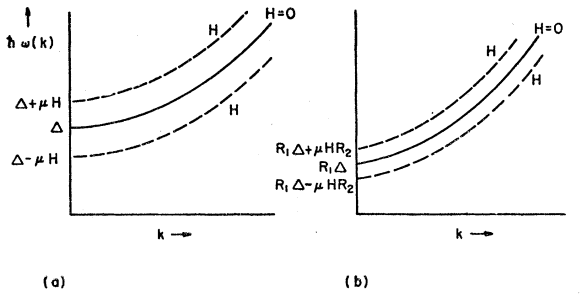

FIG. 8. Renormalization of antiferromagnetic spin-wave spectrum. (a) Simple spin-wave spectrum ($T=0$). (b) Renormalized spectrum, at higher T.

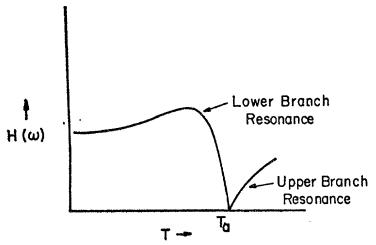

FIG. 9. Schematic of field required for AFMR as a function tion of temperature.

$R_2(\tau)$ renormalization being dominant at low T (requiring a larger field with increasing T) and the $R_1(\tau)$ renormalization being dominant at higher T.

When the $R_1(\tau)$ renormalization reduces the energy gap $R_1(\tau)\Delta$ to the signal frequency ω, the field $H(\omega)$ required for resonance becomes zero. At higher temperatures the $\mathbf{k}=0$ modes lies below $\hbar\omega$. Application of a field H then drives the *upper* branch of the curve upward to resonance, and the condition for resonance becomes

$$\mu H(\omega)=[\hbar\omega/R_2(\tau)]-[R_1(\tau)/R_2(\tau)]\Delta. \quad (10.8)$$

As the temperature increases further the separation $\hbar\omega-R_1(\tau)\Delta$ increases, and the field $H(\omega)$ increases as shown in Fig. 9, after Foner.[17]

Comparison of theory with experiment is given in Table V. The values of J and K are determined by the experimental values of the Néel temperature and by the field required for resonance at $T=0°$K, with a particular AFMR frequency. Comparison is then made of the fields required for resonance at various frequencies, at $T=0°$K, with the temperature at which the field vanishes for each frequency, and with the initial slopes of the field-versus-temperature curves. The experimental data is taken from the measurements of Foner on Cr_2O_3. The agreement, using the CD approximation, is quite good.

Turning now from the phase transitions to the thermodynamic properties of the antiferromagnetic phase, with zero external field and vanishing anisotropy, two distinct approximations (RPA and CD) have been used to determine the sublattice magnetization and the parallel and perpendicular susceptibilities. For the sublattice magnetization and parallel susceptibility both approximations agree with spin-wave theory for the principal part of the τ^2 term. However, only CD agrees with spin-wave theory for the quantum corrections to the τ^2 term (except for $S=\frac{1}{2}$).

The results for the perpendicular susceptibility differ considerably in RPA and CD. Molecular-field theory predicts a temperature-independent perpendicular susceptibility and this is precisely the RPA result. However, at $T=0$, CD is in agreement with spin-wave theory, predicting a decrease from the molecular-field value [measured by the small constant $c'+c$ of Eqs. (5.4) and (5.8)]. At low temperatures both CD and spin-wave theory indicate a decrease proportional to τ^2. According to CD, the susceptibility still has a negative slope and has the value $\mu^2 N\tau_0/2zJ\tau_N$ at the Neel temperature. The values of $\chi_{CD}{}^1/\chi_{RPA}{}^1$ at $T=0$ and at $T=T_N$ are given in Table VI. The experimental curves of MnF_2 by Stout and Griffel[26] exhibit this general type of behavior with $\chi^1(T=T_N)/\chi^1(T=0)=0.76$ as compared with our predicted value 0.92. However, we stress the fact that our approximations are not expected to be valid in the vicinity of the Néel temperature. We accordingly place more emphasis on the quantitative agreement with spin-wave theory at low temperature, and on the general agreement with experimental observations at intermediate temperatures, than on quantitative comparison with data at the Néel temperature.

TABLE VI. Ratio of perpendicular susceptibilities ($\chi_{CD}{}^1/\chi_{RPA}{}^1$) at $T=0$ [Eq. (5.17)] and at $T=T_N$ [Eq. (6.16)].

	Simple cubic		Body-centered cubic	
S	$T=0$	$T=T_N$	$T=0$	$T=T_N$
$\frac{1}{2}$	0.75	0.75	0.78	0.78
1	0.87	0.82	0.89	0.84
$\frac{3}{2}$	0.92	0.84	0.93	0.87
2	0.94	0.86	0.94	0.88
$\frac{5}{2}$	0.95	0.86	0.96	0.88
3	0.96	0.87	0.96	0.89

Further insight of the behavior of the perpendicular susceptibility may be gained by recalling that the susceptibility measures the transverse correlation function

$$\chi^1=\beta\mu^2\sum_{i,j}\langle i^x j^x\rangle. \quad (10.9)$$

The physical source of the decrease in χ^1 from the molecular-field value, at $T=0$, is the contribution of the spin-wave zero-point oscillations. These contribute primarily to the self-correlation term $i=j$, in the series (10.9). As the temperature increases, this self-correlation increases with the amplitude of the transverse spin components, but the negative nearest-neighbor correlation also builds up as longer-wavelength spin waves are excited. The competition of these correlations depends delicately on the spin-wave renormalization, giving the result

$$\chi^1=(\mu^2N/2zJ)(1-\alpha\psi_\delta)^{-1}. \quad (10.10)$$

We have specifically taken the anisotropy K to be zero in this discussion to stress that the temperature dependence of the perpendicular susceptibility is a fundamental property, quite distinct from the phenomenological temperature dependence ascribed to the anisotropy in discussions based on molecular-field theory.[32]

Finally, we note that the approximations here explored fail in the immediate vicinity of the Néel temperature. In the case of vanishing anisotropy, the apparent Néel temperatures of the paramagnetic and antiferromagnetic phase are the same in RPA, while they differ considerably in CD. The Néel temperatures predicted by RPA and CD for the antiferromagnetic

phase with zero anisotropy are in agreement with the Curie temperatures obtained for a ferromagnet of equal $|J|$, using the same approximations. This equality is in close agreement with the Padé predictions of Rushbrooke and Wood.[43] CD yields higher Néel temperatures than RPA and for the larger spin values is in better quantitative agreement with the results obtained by Rushbrooke and Wood.

ACKNOWLEDGMENTS

We express our appreciation to Dr. Raza Tahir-Kheli for many critical comments and helpful discussions, and to Professor Simeon Friedberg, of the Carnegie Institute of Technology, for an informative discussion and for making available to us before publication the measurements of John Schelleng and S. Friedberg on the phase transitions of $MnBr_2 \cdot 4H_2O$.

PHYSICAL REVIEW VOLUME 136, NUMBER 4A 16 NOVEMBER 1964

Self-Diffusion and Nuclear Quadrupolar Relaxation in fcc Lanthanum Metal*

DAVID ZAMIR† AND D. S. SCHREIBER‡
Laboratory of Atomic and Solid State Physics, Cornell University, Ithaca, New York
(Received 22 June 1964)

The nuclear magnetic-resonance spin-lattice (T_1) and spin-spin (T_2) relaxation times and the Knight shift of La^{139} in pure fcc lanthanum metal have been studied from 295 to 825°K. The relaxation times exhibit a temperature dependence which can be explained by vacancy diffusion and annealing effects that perturb the spin system via the nuclear electric-quadrupole interaction. At the highest temperatures, it is found that $T_1 = T_2 \propto \exp(E_a/kT)$ where $E_a = 15$ kcal/mole is found for the activation energy of vacancy formation and diffusion. The Knight shift is found to increase from 0.64% at 295°K to 0.72% at 825°K, which may be the result of an electron-phonon interaction.

I. INTRODUCTION

THE behavior of the nuclear spin-spin (T_2) and spin-lattice (T_1) relaxation times of La^{139} in pure fcc lanthanum metal has been studied from 25 to 550°C. The major part of their temperature dependence can be interpreted on the basis of vacancy diffusion and formation, on a competition between the two stable crystal structure forms, hcp and fcc, and annealing effects, all of which affect the nuclear-spin system via the electric-quadrupole interaction.

X-ray studies[1] have shown that hcp La metal begins to transform to an fcc structure at 200°C which is then stable even below 200°C. Cold working below 200°C restores the hcp phase. However, even in the fcc phase, a small amount of hcp phase remains.[1] The fact that the c/a ratio $(c/a)_{La} = 1.61$ of hcp La is not ideal, and that La^{139} possesses a moderate quadrupole moment, leads to a quadrupole interaction which has the effect of broadening the resonance linewidth, or alternatively of shortening T_2, while at the same time reducing the intensity of the resonance by removing the satellite transitions from the central resonance. The central resonance ($m = \frac{1}{2} \rightarrow m = -\frac{1}{2}$) and the two inner satellites ($m = |\frac{1}{2}| \leftrightarrow |\frac{3}{2}|$) have been observed[2] in hcp La which was annealed for several days at a temperature just below the phase-transition temperature. Another source for a quadrupole interaction in hcp La, which will manifest itself whenever the local symmetry is noncubic, is strains and stacking faults which are difficult to anneal away since annealing must be done below 200°C to preserve the hcp phase.

The fcc phase of La should ideally show no evidence of a static quadrupole interaction. However, any deviation from cubic symmetry such as a small amount of the hcp phase will produce an observable effect. On the other hand, even in a pure fcc phase rapidly time varying or momentary deviations from cubic symmetry as may be produced by diffusing vacancies or other defects will be observable in a T_1 (spin-lattice relaxation-time) measurement, where T_1 is considerably shortened via the quadrupolar-relaxation mechanism.

A study of the La linewidth, with some direct T_1 measurements, from 25 to 550°C reveals the effect of both a static and a time varying quadrupole interaction. Quantitative results of vacancy formation and diffusion and annealing effects are deduced and are discussed in Sec. III. A Knight shift, increasing with temperature, is also observed and is qualitatively discussed.

II. EXPERIMENTAL

In order to avoid skin-depth-effect problems, the samples were prepared in the form of a powder by using

* Supported in part by the National Science Foundation and the Advanced Research Projects Agency.
† Present address: Soreq Research Establishment, Yavne, Israel.
‡ Present address: Department of Physics, Northwestern University, Evanston, Illinois.
[1] W. T. Ziegler, R. A. Young, and A. L. Floyd, J. Am. Chem. Soc. 75, 1215 (1953).
[2] D. Torgeson, D. Peterson, and R. G. Barnes, Bull. Am. Phys. Soc. 8, 529 (1963).